# Stochastic Dual Dynamic Programming for Optimal Power Flow Problems under Uncertainty

Adriana Kiszka
TUM School of Management, Technische Universität München, 80333 Munich, Germany, adriana.kiszka@tum.de
David Wozabal
TUM School of Management, Technische Universität München, 80333 Munich, Germany, david.wozabal@tum.de

We propose the first computationally tractable framework to solve multi-stage stochastic optimal power flow (OPF) problems in alternating current (AC) power systems. To this end, we use recent results on dual convex semi-definite programming (SDP) relaxations of OPF problems in order to adapt the stochastic dual dynamic programming (SDDP) algorithm for problems with a Markovian structure, employing scenario lattices to discretize the underlying randomness. We show that the usual SDDP lower bound remains valid and that the algorithm converges to a globally optimal solution of the stochastic AC-OPF problem as long as the SDP relaxations are tight. To test the practical viability of our approach, we set up an extensive case study of a storage sitting, sizing, and operations problem under uncertainty about demand and renewable generation using the IEEE RTS-GMLC network. We show that the convex SDP relaxation of the stochastic problem is usually tight and discuss ways to obtain near-optimal physically feasible solutions when this is not the case. Using these results, we demonstrate that the algorithm finds a physically feasible policy with a small optimality gap to the original non-convex problem and yields a significant added value of 27% over a rolling deterministic planning policy.

*Key words*: Optimal power flow, semi-definite programming, stochastic dual dynamic programming, electricity storage

## 1. Introduction

The power sector is instrumental in the efforts to transition to a clean, carbon neutral energy system. In the process of this transition, power systems all over the world experience transformational change as new sources of demand like electric mobility or electric heating are gaining importance and production is increasingly shifted to variable renewable sources of electricity (VRES).

Especially the latter development increases the stress on existing power systems, since VRES capacities are often located far from demand centers and consequently induce power flows that existing transmission systems were not designed for. Furthermore, the output of wind energy and solar PV, the most common forms of renewable power generation, is intermittent and depends on

environmental factors outside the control of plant owners and transmissions system operators.

As a result there are numerous new challenges in the design and operation of power networks and it is presently unclear how to best resolve them in a manner that leads to reliable electricity systems and at the same time is cost efficient. In particular, the question of how and to which extent existing grid infrastructure has to be updated and what role grid-level electricity storage should play is central to planning and operating future power systems.

In order to answer these questions, one has to take into account the physical laws of power flow and solve optimal power flow (OPF) problems, i.e., optimization problems that incorporate explicit rules governing physical power flows in their constraints or their objective functions. The goal of OPF problems is to optimize the steady-state operating point of transmission and distribution networks in order to deliver electricity from suppliers to consumers as efficiently as possible. This fundamental problem was formulated for the first time by Carpentier (1962) and since then substantial developments have been made in the understanding of this problem class. See Frank et al. (2012a,b), Wang and Hijazi (2018) for excellent surveys of the recent literature.

While direct current (DC) networks can be incorporated relatively easily in optimization models through a set of linear constraints, networks with alternating current (AC) require non-linear constraints that make the resulting AC-OPF problems non-convex and ultimately NP-hard (e.g. Lavaei and Low 2012).

However, real-world energy systems use alternating current, since AC power can be easily *stepped up and down* between different voltage levels enabling the parallel operation of a long-distance, high-voltage transmission system and a distribution grid, which provides safe low voltage electricity to end consumers.

Many standard planning tools, used for example by network operators, ignore the complexities of AC power flow and employ DC relaxations of AC-OPF problems. While these approximations work well for the high-voltage transmission system where voltage angles do not play a big role, they lead to large deviations from physical realities in lower voltage grids (see, e.g., Stott et al. 2009, Larrahondo et al. 2021).

Additionally, there are many other tractable approximations that can be used solve AC-OPF problems including various linear programming based relaxations and approximations as in Castillo et al. (2016b), Coffrin and Van Hentenryck (2014), Shchetinin et al. (2018), local search algorithms Bukhsh et al. (2013b), Wu et al. (2018a), and a variety of conic relaxations (e.g., Low 2014a,b).

In classic power systems planning the only sources of uncertainty are conventional demand and power plant outages. Since in large networks the former can be very well predicted and the latter is a rare event that is taken care off by redundancies in network design, traditional OPF problem formulations are usually deterministic. However, the transition to carbon neutral power systems

that rely on many distributed resources and encompass an increasing share of load from electric heating and electric mobility introduces new sources of uncertainty, changing the nature of OPF problems and necessitating a more explicit treatment of randomness.

In particular, the large-scale introduction of VRES such as wind power or solar PV introduce uncertainty on the supply side which is absent from classical power systems planning. Furthermore, as the potential for demand response by small dispersed consumers keeps increasing with the introduction of smart grids, electric heating, and electric mobility, the resulting flexibilities can be used by grid operators. Making use of this flexibility entails dealing with resources that are only partly in control of the system operator and whose availability and operational state have to be considered as uncertain at the time of planning.

In this paper, we propose a general multi-stage stochastic optimization framework for AC-OPF problems that explicitely models AC power flow and at the same time is computationally tractable. In particular, we show that recent advances in convex relaxations of AC-OPF problems and decomposition methods for Markovian stochastic optimization problems can be combined to generate high-quality, physically accurate solutions for multi-stage stochastic AC-OPF problems.

Since even linear two-stage stochastic optimization, the most well behaved subclass of stochastic optimization problems, is NP-hard (Hanasusanto et al. 2016), solving stochastic multi-stage AC-OPF problems seems hopeless at first glance.

Nevertheless, some attempts have been made to solve stochastic AC-OPF problems in the extant literature. However, most approaches consider two-stage stochastic optimization problems (e.g. Mühlpfordt et al. 2016, Bai et al. 2017, Sharifzadeh et al. 2017, Bucciarelli et al. 2018, Roald and Andersson 2018, Mezghani et al. 2020) and most authors additionally use DC approximations (e.g., Oh 2011, Zhang and Li 2011, Vrakopoulou et al. 2013, Cao et al. 2013, Bienstock et al. 2014, Pandzic et al. 2015, Zhang et al. 2017). These models typically combine an investment decision on the first stage with operational decisions, possible over a longer period of time, in the second stage.

However, multi-stage stochastic programming, where uncertainty gradually *reveals itself* over several stages, is important for operational planning in systems containing assets that *link* several time periods, such as electricity storage. Models that merge operational planning into a single stage implicitly assume perfect information, which is overly optimistic and typically leads to underinvestment in storage and line capacity.

The literature on multi-stage stochastic optimization in OPF problems is extremely scarce. In fact, to the best of our knowledge, the only truly multi-stage stochastic OPF problem is proposed in Xiong and Singh (2016) who solve a stochastic storage sitting, sizing, and operation problem with wind generation uncertainty using a scenario tree and DC power flow approximations.

In our approach, we utilize recent advances in convex semi-definite programming (SDP) relaxations of AC-OPF problems that have been shown to allow for fast and accurate solutions of deterministic problems. In particular, the seminal paper Lavaei and Low (2012) uses the dual of a relaxed SDP formulation of a specific AC-OPF problem and demonstrate that after some small modifications to the admittance matrix, which do not change the problem in a practically meaningful way, the approximation is tight for a large range of problems.

These results triggered a flurry of research in refined conic approximations in, e.g., Low (2014a), Madani et al. (2016), Coffrin et al. (2017), further relaxations to second order cone programming in Jabr (2006), Kocuk et al. (2016b), quadratic programming in Coffrin et al. (2016), Marley et al. (2017), linear programming in Misra et al. (2018) or mixed-integer programming Bienstock and Muñoz (2014). Since the SDP relaxations are not always exact (e.g., Bukhsh et al. 2013b, Molzahn et al. 2016), numerous authors focus on tightening them. Examples include branch-and-bound algorithms to iteratively partition the feasible set of relaxations in order to find a solution with a smaller gap (Chen et al. 2016, Phan 2012). In Madani et al. (2015b) and Natarajan et al. (2013) penalization terms are incorporated into the objective to ensure the feasibility of solutions produced by relaxation. Josz et al. (2015), Molzahn and Hiskens (2015c) propose employing moment-based hierarchies to form conic relaxations that result in globally optimal solutions for AC-OPF problems. Andersen et al. (2014), Molzahn et al. (2013) leverage the sparsity of power networks through a tree decomposition of the problem. Further work in this direction uses valid inequalities as in Kocuk et al. (2016b), cutting planes in Kocuk et al. (2018), convex envelopes in Coffrin et al. (2017), and sequential and bound-tightening methods in Wei et al. (2017), Schetinin (2019). We refer to Molzahn and Hiskens (2019), Zohrizadeh et al. (2020) for a comprehensive overview of this very active field of research.

Another important building block of our approach are the advances in decomposition methods for multi-stage stochastic optimization that make it possible to solve large convex Markovian problems with many stages in relatively short time. One of the most successful algorithmic frameworks in this regard is *stochastic dual dynamic programming* (SDDP), which decomposes stochastic optimization problems along its stages and was originally proposed for problems with stage-wise independent randomness in Pereira and Pinto (1991).

Since then the original SDDP algorithm has been considerably refined and is now very well understood. In particular, Philpott and de Matos (2012), Löhndorf et al. (2013), Löhndorf and Wozabal (2021) extend the original SDDP method to Markovian processes and Kiszka and Wozabal (2020) propose a semi-metric that allows to quantify the error made by approximating general Markov processes by discrete scenario lattices.

Convergence of SDDP is studied in Philpott and Guan (2008) for the linear case and in Girardeau et al. (2015) for a fairly general class of convex problems. Furthermore, Löhndorf et al. (2013) relax some of the restrictions of the original version of the method and Shapiro (2011) studies probabilistic stopping criteria. Terça and Wozabal (2020) show how to compute sensitivities for stochastic optimization problems solved using SDDP and propose an asymptotic approximation error of lattice based approximations.

Finally, Lan (2020) shows that the complexity of SDDP only grows polynomially in the number of stages and therefore curbs the *curse of dimensionality* for stochastic optimization problems where the main difficulty are not large decision problems in the stages but rather the fact that there are many decision stages.

The contribution of this paper, can be summarized as follows:

1. We propose an SDDP decomposition algorithm for a general class of multi-stage stochastic AC-OPF problems by combining recent results on SDDP for Markovian multi-stage stochastic optimization problems based on scenario lattices with results on convex SDP relaxation of AC-OPF problems. The result is a general framework that can be used to solve a large class of multi-stage AC-OPF problems.
2. We show that the proposed algorithm converges to the true solution, if the relaxation of the AC-OPF problems on the nodes of the scenario lattices are exact in the forward pass and the backward pass of the algorithm. Furthermore, we show that the gap between the SDDP upper and lower bound can be used as a certificate of convergence, as long as physically feasible voltages can be found in the forward pass. To that end, we propose a method to compute such physically feasible solutions as *projections* of the solutions of the relaxed AC-OPF problem to the feasible set of the non-convex problem in cases where the employed convex relaxation is not tight.
3. We provide a proof of concept in the form of an extensive storage sitting, sizing, and operations problem in a modified version of the network proposed in Barrows et al. (2020). We model renewable production by wind and solar as well as loads as random and decide about storage investments in the first stage and about operation for a consecutive week of planning in the later stages.

   The results illustrate that the problem can be solved in reasonable time with an optimality gap of below 3% relative to the globally optimal policy. We furthermore demonstrate that the stochastic approach yields significantly different policies than rolling deterministic planning, which leads to lower investment in storage and consequently more curtailment of production and loads as well as higher cost resulting in a significant value of the stochastic solution of 27%.

The rest of the manuscript is organized as follows: In Section 2, we give a short, yet self-contained, introduction to AC-OPF problems and their formulation as semi-definite programs, which is complemented by an appendix that provides more details on the construction of admittance matrices. In Section 3, we integrate the dual of a relaxed AC-OPF problem with the SDDP algorithm and give sufficient conditions for convergence to the true solutions of the non-convex problem. Section 4 is devoted to the storage sitting, sizing, and operations problem which explores the computational aspects of the proposed approach in a medium-sized application example. Finally, Section 5 concludes the paper and discusses avenues for further research.

*Notation*: We work on a standard probability space $(\Omega, \mathcal{F})$ and define a filtration $\{\emptyset, \Omega\} = \mathcal{F}_0 \subseteq \mathcal{F}_1 \subseteq \cdots \subseteq \mathcal{F}_T \subseteq \mathcal{F}$ such that all random quantities $\xi_t$ that realize in period $t$ are measurable with respect to $\mathcal{F}_t$, denoted by $\xi_t \triangleleft \mathcal{F}_t$. We denote by $\mathbb{S}^d$ the set of symmetric $(d \times d)$ matrices. Furthermore, $x \circ y$ denotes the element-wise multiplication of two vectors $x$ and $y \in \mathbb{R}^d$, while $A \bullet B = \operatorname{tr}(AB)$ with $\operatorname{tr}(A)$ the trace of a matrix $A$. Lastly, we use the notation $[d] = \{1, \ldots, d\}$ for $d \in \mathbb{N}$, denote complex conjugation by $^*$, and the conjugate transpose by $^H$.

## 2. Problem description

In this section, we specify a class of fairly general finite-horizon multi-stage AC-OPF problems. Section 2.1 features a brief introduction to the relevant principles of AC power flow. For an in-depth treatment of the fundamentals of power flow, we refer to Glover et al. (2008), while Frank and Rebennack (2016) give a compact yet excellent introduction to the subject of optimal power flow problems. In Section 2.2 these principles are applied to power system modeling. Section 2.3 uses these preparations to define a multi-stage stochastic AC-OPF problem in its extensive form. Finally, in the spirit of Lavaei and Low (2012), Section 2.4 introduces an SDP formulation of the AC-OPF problem, which naturally lends itself to a convex approximation.

### 2.1. Alternating Current Power Flow

In a direct current circuit voltage remains constant over time. In this setting all features of the system relevant to this paper can be explained with the *water analogy*, where *electric charge* is equated to water flowing between reservoirs of different elevation which correspond to nodes of the electrical circuit. Gravity induces a potential between the reservoirs, which corresponds to *voltage* $V \in \mathbb{R}$ and represents the potential energy per unit of water/charge, while the flow of water equals *electric current* $I \in \mathbb{R}$. Lastly, the limited diameter of the pipes connecting the reservoirs introduces an opposition to flow which has an effect that is analogous to *electric resistance* $R \in \mathbb{R}$. Note that $V$ is a *difference in potential*, i.e., voltages relate different nodes of a circuit. If voltages are associated

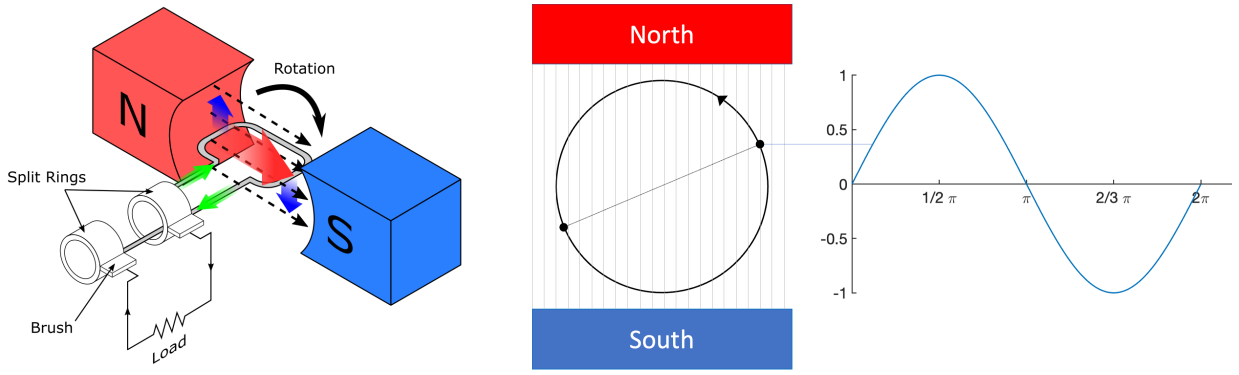


**Figure 1** The left panel shows a simplified design of an AC generator where a looped conductor is rotated in a magnetic field by an external force (image by courtesy of `www.saVRee.com`). The right panel shows a cut through the generator on the right with the two dots representing the wire and the induced sinusoidal voltage wave on the right.

to single nodes, they are to be interpreted as differences to the system reference, usually *ground*, i.e., the lowest possible voltage level of no electric potential at all.

Bearing in mind this analogy, Ohm's law, $V = IR$, stating that for a given *voltage/pressure*, the induced *current/flow* is inverse proportional to the resistance, makes intuitive sense. Furthermore, it is easy to comprehend *Kirchhoffs current law*, which states that the current flowing into a node from connected nodes equals the current flowing out of the node (no current/water is lost) as well as the *Kirchhoffs' voltage law*, which requires voltages (elevation differences) to sum to zero when going around a closed loop in the network. These ingredients are sufficient to *solve* DC networks, i.e., calculate all unknown voltages and currents, using linear equations that can be easily incorporated in convex optimization problems.

Alternating current networks differ from the DC situation in that voltages follow a sinusoidal pattern $v(t) = V^A \sin(2\pi wt + \phi)$ over time $t$, where $V^A$ is the peak voltage, $\phi$ is the phase angle, and $w$ is the frequency in Hertz (if time is measured in seconds). This pattern is induced by AC voltage sources, which typically come in the form of generators that transform mechanical energy into electric energy by rotating a coiled wire in a magnetic field in a circular motion with constant angular speed as illustrated in Figure 1. Since moving a conductor in a magnetic field produces voltage in the conductor that is proportional to the speed at which the coil crosses the magnetic field lines, i.e., the horizontal speed of the conductor in the right panel of Figure 1, the induced voltage follows a sinusoidal pattern. Note that as the two parts of the coil change positions the voltage differences change sign due to *Flemming's right hand rule*.

Since voltages and currents are fluctuating in AC systems, they are usually described in terms

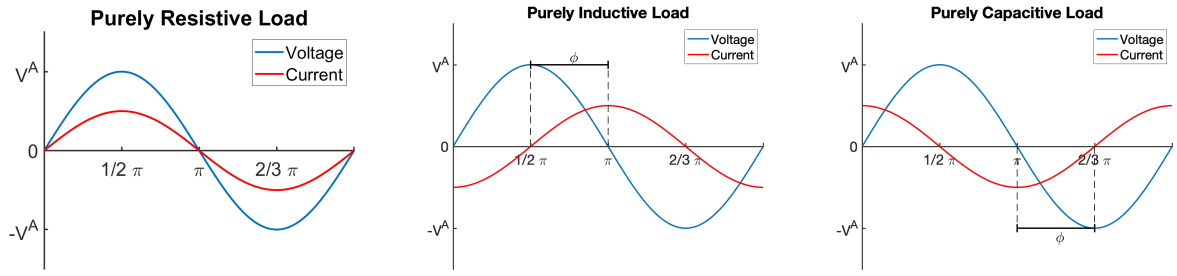


**Figure 2** Three types of loads which represent the different opposition to current flow in AC circuits assuming the phase angle of the voltage to be equal to zero. The first panel shows a purely resistive load with voltage and current in phase, the second panel shows a purely inductive load with a negative phase angle of $\phi = -\pi/2$ (the current *leads* the voltage), while the last panel shows a purely capacitive load with a positive phase angle of $\phi = \pi/2$ (the current *lags* the voltage).

of either their peak values $V^A$ or, more commonly, their *root mean square* (RMS) values which, in case of the voltage, are defined as

$$V^{RMS} = \sqrt{\int_0^1 \left(V^A \sin(2\pi wt + \phi)\right)^2 dt} = V^A \sqrt{\int_0^1 \sin(2\pi wt)^2 dt} = \frac{V^A}{\sqrt{2}}.$$

The definition of $I^{RMS}$ for currents $i(t)$ is analogous.

While in DC network the only *opposition to current flow* is resistance, the pulsating nature of AC voltage induces another type of opposition, which is called *reactance*. Reactance is caused by charge being stored either in magnetic fields which form around coils in electric components such as motors or transformers (*inductive reactance*) or on the plates of a capacitor (*capacitive reactance*). In case of the more common inductive reactance, the magnetic field lines cross the coil as the voltage in the network rises and the field builds up, inducing a current in the opposite direction of the current supplied by the voltage source. This is a manifestation of the same electromagnetic principle by which a voltage is induced when a coil moves through the magnetic field in a generator.

Both inductive and capacitive reactance thus *disturb* the current flow $i(t)$ and cause it to be *out of phase* with the voltage that is produced by the voltage source as shown in Figure 2. In reality, loads are never purely resistive, inductive, or capacitive but rather present themselves as a mixture of these effects which together result in a cumulative phase shift $\phi \in [-\pi/2, \pi/2]$ of the current $i(t)$ relative to the voltage $v(t)$. However, the current can always be decomposed by projection on a purely resistive component (in phase with the voltage) and a component that is purely reactive/capacitive (completely out of phase) in the Hilbert space of square integrable functions.

As in DC networks, in AC networks, the instantaneous power at time $t$ is the product of voltage and current, i.e., $p(t) = v(t)i(t)$. Assuming without loss of generality that the phase angle of the voltage is zero and $i(t) = I^A \sin(2\pi wt + \phi)$, results in a cumulative power production of

$$\begin{aligned} P &= V^A I^A \int_0^1 \sin(2\pi wt)\sin(2\pi wt + \phi)dt \\ &= V^A I^A \left(\cos(\phi)\int_0^1 \sin(2\pi wt)^2 dt + \sin(\phi)\int_0^1 \sin(2\pi wt)\cos(2\pi wt)dt\right) \\ &= V^A I^A \cos(\phi)\int_0^1 \sin(2\pi wt)^2 dt = V^{RMS} I^{RMS}\cos(\phi) \end{aligned} \tag{1}$$

in one unit of time, which is called *active power* and represents the amount of useful electrical work delivered to the system. Note that due to the phase shift the second term in (1) occurs, which represents the wastage of energy due to reactance in the network and which at times produces *negative power flows*, reducing the overall useful energy in the circuit. Taking the absolute value of these flows results in $V^{RMS} I^{RMS}\sin(\phi)$, which is called *reactive power* $Q$.

These relationships are frequently described by representing voltages, currents, and powers as complex numbers. Taking the example of currents, the idea is to represent $i(t) = I^A \sin(2\pi wt + \phi_I)$ by the complex number $I = I^{RMS} e^{i\phi_I}$, which encodes both the magnitude and the phase angle. Using this notation and setting the phase angle of the voltage to $\phi_V$, we can write active and reactive power as

$$P = \mathfrak{Re}(VI^*) = \mathfrak{Re}(V^{RMS} I^{RMS} e^{i(\phi_V - \phi_I)}),\ Q = \mathfrak{Im}(VI^*), \tag{2}$$

which are the real and imaginary part of complex power $S = VI^* = P + iQ$, respectively. Note that the *apparent power* $|S|$ is the amount of energy that has to be put into the system, e.g., in the form of mechanical energy turning the generator. Hence, active, reactive and apparent power are related by the *pythagorean relationship* $|S|^2 = P^2 + Q^2$, which is usually referred to as the *power triangle*, imagining the components $P$, $Q$, and $S$ as the sides of a right angled triangle with angle $\phi = (\phi_V - \phi_I)$ between the hypotenuse $|S|$ and the side $P$. We remark that reactive power $Q$ has no physical manifestation but merely represents the loss of power induced by reactance according to the abovementioned relationship.

Note that Ohm's law which relates voltages, currents, and resistance, can be generalized to AC circuits by writing $V = IZ$ where $Z$ is the complex *impededance* $Z = |Z|e^{i\phi} = R + iX$ with $R$ being classic resistance and $X$ being the reactance. Multiplying complex current with impedence therefore does not only have a scaling effect (as in the DC case), but, by the choice of a non-zero reactance, also causes a rotation by $\phi$ which allows to model the phase-shifting effect of reactance. Equivalently, we can write $I = VY$, where $Y = Z^{-1}$ is called the *admittance*.

We conclude our introduction to AC power flow, by noting that the fact that relevant quantities in AC networks, such as active and reactive power in (2) depend in non-convex ways on the phase angles through the sine and cosine functions makes AC-OPF problems non-convex and usually NP-hard (Lavaei and Low 2012).

### 2.2. Network Modeling

Electrical power systems are modeled as a network of $n$ buses $\mathcal{N} = \{1, 2, \ldots, n\}$ which are interconnected by branches (lines) $\mathcal{L} \subseteq \mathcal{N} \times \mathcal{N}$. A bus corresponds to a node in a circuit and represents a load center (such as a lower voltage subnetwork), a generation unit, or a connection point to a higher voltage grid.

We associate to every bus $k \in \mathcal{N}$ a voltage $V_k \in \mathbb{C}$ relative to the system reference, usually ground, a current $I_k$ which is absorbed/produced in the bus, and a shunt admittance $y_k$ which models the admittance to bus. Furthermore, each branch $(l, m) \in \mathcal{L}$ has an associated series admittance $y_{lm} \in \mathbb{C}$ modeling the impedance of the branch.

Note that by Kirchhoff's current law and Ohm's law, we get for every node $k \in \mathcal{N}$

$$0 = y_k(V_k - V_{k0}) + \sum_{i \neq k} y_{ki}(V_k - V_i) \Leftrightarrow I_k = y_k V_k + \sum_{i \neq k} y_{ki}(V_k - V_i),$$

where $V_{k0}$ is the bus voltage and the first term therefore is the flow of current into/out of the bus while the second term is the flow from other buses. In order to represent these relationships in a parsimonious form, we organize voltages and currents in vectors $V = (V_1, \ldots, V_n)^\top$ and $I = (I_1, \ldots, I_n)^\top$ and define a so called *admittance matrix* $Y$ with elements

$$(Y)_{kj} = \begin{cases} y_k + \sum_{i \neq k} y_{ki}, & k = j \\ -y_{kj}, & k \neq j, \end{cases}$$

so that we can express the relationship between currents and voltage vectors as $I = YV$.

In a real network, the computation of the admittance matrix is complicated by the need to account for shunt admittances of lines and possibly the existence of phase-shifting transformers with off-nominal turns ratios. We refer to Appendix B for details.

With these preparations, we can state AC-OPF problems entirely in terms of voltage and power, writing

$$S = V \circ I^* = V \circ Y^* V^*,\ P = \mathfrak{Re}(S),\ Q = \mathfrak{Im}(S) \tag{3}$$

for the vector of complex, active, and reactive powers at the buses of the network.

In order to describe flow on lines, let $e_k \in \mathbb{R}^n$ be the standard basis vectors and define the *partial admittance matrices* $Y_{lm} = (e_l e_l^\top - e_l e_m^\top) y_{lm}$, which allow to write the currents $I_{lm}$ and powers $S_{lm}$, $P_{lm}$, and $Q_{lm}$ flowing on line $(l, m) \in \mathcal{L}$ as

$$I_{lm} = y_{lm}(V_l - V_m) = e_l^\top Y_{lm} V,\ S_{lm} = V_l I_{lm}^* = V^\top Y_{lm}^* V^*,\ P_{lm} = \mathfrak{Re}(S_{lm}),\ Q_{lm} = \mathfrak{Im}(S_{lm}). \tag{4}$$

Similarly, we define the matrices $Y_k = e_k e_k^\top Y$ containing only the k-th row of $Y$ such that $I_k = e_k^\top Y_k V$.

Lastly, we remark that in power system analysis, electrical quantities are usually expressed in a *per unit system* as a ratio of the actual SI quantity to a base quantity. The per unit values are easier to interpret, as they usually lie within a narrow numerical range close to 1. Furthermore, the per unit system improves the numerical stability of power flow calculations and reduces serious calculation errors, e.g., when referring quantities from one side of a transformer to the other.

### 2.3. A Stochastic Optimal Power Flow Problem

Optimal power flow problems are optimization problems that include the physical rules for power flow in their constraints or objectives. Classic formulations minimize the cost of electricity generation while maintaining the power system within safe operating limits.

We propose a general formulation of a finite horizon multi-stage stochastic AC-OPF problem. To this end, we assume that the part of the problem that is not directly concerned with modeling the power flow can be formulated as an SDP, thus covering most convex problem formulations of interest.

We denote the set of time periods by $t \in \mathcal{T} = \{1, \dots, T\}$ and organize the non-electrical decision variables that model decisions taken in stage $t$ into the symmetric, positive semi-definite matrix $X_t \in \mathbb{S}^{d_t}$, which may, for example, contain investment, operational, as well as trading and financial decisions.

We define the objective function as the expected cost over all stages

$$\mathbb{E}\left[\sum_{t\in\mathcal{T}} F_t \bullet X_t\right],$$

where $F_t : \Omega \to \mathbb{S}^{d_t}$ are random symmetric matrices with $F_t \triangleleft \mathcal{F}_t$. Note that the formulation above does not only cover risk-neutral decision making but, by a suitable definition of variables and constraints, can also accommodate the most-common risk measures (see, e.g., Föllmer and Schied 2004, Pflug and Römisch 2007).

We impose the following set of $s_t \in \mathbb{N}$ constraints in every stage of the problem

$$A^1_{ti} \bullet X_{t-1} + A^2_{ti} \bullet X_t \le a_{ti}, \quad \forall i \in [s_t],\, t \in \mathcal{T}, \tag{5}$$

where $A^1_{ti}, A^2_{ti} : \Omega \to \mathbb{S}^{d_t}$ and $a_{ti} : \Omega \to \mathbb{R}$ are random data with $A^1_{ti}, A^2_{ti}, a_{ti} \triangleleft \mathcal{F}_t$. As in standard stochastic optimization formulations, for example for two-stage stochastic optimization problems (Birge and Louveaux 2011), (5) serves two purposes: Firstly, it models the constraints on decision variables in one stage of the problem and secondly, it can be used to relate the variables in stage

$t-1$ with the variable in stages $t$, thereby defining the dynamics of the problem on the level of the decisions. In this sense, the matrices $A^1_{ti}$ take the role of the *recourse matrix* in classic multi-stage linear stochastic programming.

Apart from $X_t$, the model also contains the voltages $V_{tk}$, the complex powers $S_{tk}$, the active powers $P_{tk}$, and the reactive powers $Q_{tk}$ for bus $k$ in time period $t$ as decision variables. In order to model the physical behavior of the electrical system, we impose the following constraint

$$S_t = V_t \circ Y_t^* V_t^*,\ P_t = \mathfrak{Re}(S_t),\ Q_t = \mathfrak{Im}(S_t), \tag{6}$$

which relates voltages and powers on all buses of the network. In order to connect the decisions $X_t$ to these variables, we impose the constraints

$$P_{tk} = A^P_{tk} \bullet X_t + a^P_{tk}, \qquad \forall k \in \mathcal{N}, t \in \mathcal{T} \tag{7}$$

$$Q_{tk} = A^Q_{tk} \bullet X_t + a^Q_{tk}, \qquad \forall k \in \mathcal{N}, t \in \mathcal{T}. \tag{8}$$

where $A^P_{ti}, A^Q_{ti} : \Omega \to \mathbb{S}^{d_t}$ and $a^P_{ti}, a^Q_{ti} : \Omega \to \mathbb{R}$ are random. The above constraints model inflows and outflows of power in the form of (possibly random) generation or random load and ensure that the electric variables modeling the power flow are in line with the decisions $X_t$, which determine how much power is injected/withdrawn in each bus.

Furthermore, we make the upper bounds for active power $P_{tlm}$, apparent power $S_{tlm}$, and voltage differentials between busses that are connected by branches $(l, m)$ dependent on the decisions $X_t$

$$|P_{tlm}| \le B^P_{tlm} \bullet X_t + b^P_{tlm}, \qquad \forall (l,m) \in \mathcal{L}, t \in \mathcal{T} \tag{9}$$

$$|S_{tlm}|^2 \le B^S_{tlm} \bullet X_t + b^S_{tlm}, \qquad \forall (l,m) \in \mathcal{L}, t \in \mathcal{T} \tag{10}$$

$$|V_{tl} - V_{tm}|^2 \le B^V_{tlm} \bullet X_t + b^V_{tlm}, \qquad \forall (l,m) \in \mathcal{L}, t \in \mathcal{T}, \tag{11}$$

with random symmetric coefficient matrices $B^P_{tlm}$, $B^S_{tlm}$, $B^V_{tlm}$ and random parameters $b^P_{tlm}$, $b^S_{tlm}$, and $b^V_{tlm}$. Note that as these quantities are highly dependent on one another, most power flow models feature only one set of the above constraints.

Putting everything together we arrive at the following multi-stage stochastic optimization problem for which we assume all constraints to hold almost surely.

$$\begin{aligned}
&\min\ \mathbb{E}\left[\sum_{t\in\mathcal{T}} F_t \bullet X_t\right] \\
&\text{s.t.}\ \ (4), (6), \quad \forall t \in \mathcal{T} && \text{(power flow)} \\
&\qquad P_t, Q_t, V_t, P_{tlm}, S_{tlm} \triangleleft \mathcal{F}_t, \quad \forall t \in \mathcal{T}, (l,m) \in \mathcal{L} && \text{(non-anticipativity)} \\
&\qquad (7), (8), (9), (10), (11) && \text{(connection with } X_t\text{)} \\
&\qquad (5), X_t \succeq 0,\ X_t \triangleleft \mathcal{F}_t, \quad \forall t \in \mathcal{T}. && \text{(constraints on } X_t\text{)}
\end{aligned} \tag{12}$$

Note that the measurability constraints enforce the non-anticipativity of the decisions.

### 2.4. An SDP Reformulation

In this section, we will cast (12) as an SDP. To achieve this, we need to write the problem entirely in terms of real numbers and reformulate power flow constraints.

Following the approach in Lavaei and Low (2012), we write

$$M_k = \begin{pmatrix} e_k e_k^\top & 0 \\ 0 & e_k e_k^\top \end{pmatrix},\ M_{lm} = \begin{pmatrix} (e_l - e_m)(e_l - e_m)^\top & 0 \\ 0 & (e_l - e_m)(e_l - e_m)^\top \end{pmatrix}.$$

Furthermore, for a matrix $A \in \mathbb{C}^{n\times n}$, we define $\mathbb{A}, \hat{\mathbb{A}} \in \mathbb{R}^{2n\times 2n}$ as

$$\mathbb{A} = \frac{1}{2}\begin{pmatrix} \mathfrak{Re}(A + A^\top) & \mathfrak{Im}(A^\top - A) \\ \mathfrak{Im}(A - A^\top) & \mathfrak{Re}(A + A^\top) \end{pmatrix},\ \hat{\mathbb{A}} = -\frac{1}{2}\begin{pmatrix} \mathfrak{Im}(A + A^\top) & \mathfrak{Re}(A - A^\top) \\ \mathfrak{Re}(A^\top - A) & \mathfrak{Im}(A + A^\top) \end{pmatrix},$$

which we use to define matrices $\mathbb{Y}_k$, $\hat{\mathbb{Y}}_k$, $\mathbb{Y}_{lm}$, and $\hat{\mathbb{Y}}_{lm}$. We then define $\tilde{y} = [\mathfrak{Re}(y)^\top, \mathfrak{Im}(y)^\top]^\top \in \mathbb{R}^{2n}$ for $y \in \mathbb{C}^n$ and note that for $A \in \mathbb{C}^n$ and $y_1,\ y_2 \in \mathbb{C}^n$, we get

$$\widetilde{Ay_1} = \begin{pmatrix} \mathfrak{Re}(A) & -\mathfrak{Im}(A) \\ \mathfrak{Im}(A) & \mathfrak{Re}(A) \end{pmatrix} \tilde{y}_1, \text{ and } \mathfrak{Re}(y_1^\top y_2) = \widetilde{(y_1^*)} y_2. \tag{13}$$

To reformulate the problem, define $\tilde{V}_t$ as a real valued version of the voltage vector and $W_t = \tilde{V}_t \tilde{V}_t^\top \in \mathbb{R}^{2n\times 2n}$. The idea of the employed SDP reformulation is to transfer the problem in to the real numbers by using $\tilde{V}_t$ and then reformulate such that relevant quantities can be written as a the product $\bullet$ of $W_t$ with matrices that are derived from the admittance matrix. We demonstrate this principle using the example of active power at time $t$ in node $k$, which we can write as

$$\begin{aligned} P_{tk} &= \mathfrak{Re}(V_{tk}^* I_{tk}) = \mathfrak{Re}\left(V_t^H e_k e_k^\top I_t\right) = \mathfrak{Re}\left(V_t^H Y_k V_t\right) = \tilde{V}_t^\top \begin{pmatrix} \mathfrak{Re}(Y_k) & -\mathfrak{Im}(Y_k) \\ \mathfrak{Im}(Y_k) & \mathfrak{Re}(Y_k) \end{pmatrix} \tilde{V}_t \\ &= \tilde{V}_t^\top \mathbb{Y}_k \tilde{V}_t = \operatorname{tr}(\tilde{V}_t^\top \mathbb{Y}_k \tilde{V}_t) = \operatorname{tr}(\mathbb{Y}_k \tilde{V}_t \tilde{V}_t^\top) = \operatorname{tr}(\mathbb{Y}_k W_t) = \mathbb{Y}_k \bullet W_t, \end{aligned}$$

where the fourth equality gets rid of complex numbers and uses (13), the fifth uses $x^\top A x = \frac{1}{2} x^\top (A + A^\top) x$, while the subsequent steps use the properties of the trace operator.

The following lemma from Lavaei and Low (2012) executes this program for all relevant electrical quantities. We give a detailed proof in Appendix A.1.

Lemma 1. *For every time $t \in \mathcal{T}$, every node $k \in \mathcal{N}$, and every branch $(l, m) \in \mathcal{L}$ the following relationships hold:*

$$\begin{aligned} Q_{tk} &= \hat{\mathbb{Y}}_k \bullet W_t, & |V_{tk}|^2 &= M_k \bullet W_t \\ |I_{tlm}|^2 &= \mathbb{Y}_{lm}^\top \mathbb{Y}_{lm} \bullet W_t, & P_{tlm} &= \mathbb{Y}_{lm} \bullet W_t \\ |S_{tlm}|^2 &= (\mathbb{Y}_{tlm} \bullet W_t)^2 + (\hat{\mathbb{Y}}_{lm} \bullet W_t)^2, & |V_{tl} - V_{tm}|^2 &= M_{lm} \bullet W_t. \end{aligned}$$

Using the above result, we can reduce the power flow part of the problem to a decision about a positive semi-definite matrix $W_t$ with rank one. Since every such matrix can be uniquely factored as $W_t = \tilde{V}_t \tilde{V}_t^\top$ for a vector $\tilde{V}_t \in \mathbb{R}^{2n}$, the voltages and hence all the other electrical variables can be recovered from $W_t$.

Using the identities in Lemma 1, we can now reformulate the multi-stage stochastic programming problem as

$$
\begin{aligned}
\min\ & \mathbb{E}\left[\sum_{t\in\mathcal{T}} F_t \bullet X_t\right] \\
\text{s.t.}\ & \mathbb{Y}_k \bullet W_t = A^P_{tk} \bullet X_t + a^P_{tk}, && \forall k \in \mathcal{N},\ \forall t \in \mathcal{T} \\
& \hat{\mathbb{Y}}_k \bullet W_t = A^Q_{tk} \bullet X_t + a^Q_{tk}, && \forall k \in \mathcal{N},\ \forall t \in \mathcal{T} \\
& M_k \bullet W_t = A^V_{tk} \bullet X_t + a^V_{tk}, && \forall k \in \mathcal{N},\ \forall t \in \mathcal{T} \\
& \mathbb{Y}_{lm} \bullet W_t \le B^P_{tlm} \bullet X_t + b^P_{tlm}, && \forall (l,m) \in \mathcal{L},\ \forall t \in \mathcal{T} \\
& \begin{bmatrix} -B^S_{tlm} \bullet X_t - b^S_{tlm} & \mathbb{Y}_{lm} \bullet W_t & \hat{\mathbb{Y}}_{lm} \bullet W_t \\ \mathbb{Y}_{lm} \bullet W_t & -1 & 0 \\ \hat{\mathbb{Y}}_{lm} \bullet W_t & 0 & -1 \end{bmatrix} \preceq 0, && \forall (l,m) \in \mathcal{L},\ \forall t \in \mathcal{T} \\
& M_{lm} \bullet W_t \le B^V_{tlm} \bullet X_t + b^V_{tlm}, && \forall (l,m) \in \mathcal{L},\ \forall t \in \mathcal{T} \\
& A^1_{ti} \bullet X_{t-1} + A^2_{ti} \bullet X_t \le a_{ti}, && \forall i \in [s_t],\ \forall t \in \mathcal{T} \\
& X_t \succeq 0,\ W_t \succeq 0,\ W_t \lhd \mathcal{F}_t,\ X_t \lhd \mathcal{F}_t,\ \operatorname{rank}(W_t) = 1, && \forall t \in \mathcal{T}.
\end{aligned}
\tag{$\mathcal{P}^{nc}$}
$$

where due to the Schur's complement formula the constraint imposing negative semi-definiteness is equivalent to $(B^S_{tlm} \bullet X_t + b^S_{tlm}) \ge 0$ and

$$
\begin{aligned}
0 &\le B^S_{tlm} \bullet X_t + b^S_{tlm} - [-\mathbb{Y}_{lm} \bullet W_t, -\hat{\mathbb{Y}}_{lm} \bullet W_t][-\mathbb{Y}_{lm} \bullet W_t, -\hat{\mathbb{Y}}_{lm} \bullet W_t]^\top \\
&= B^S_{tlm} \bullet X_t + b^S_{tlm} - (\mathbb{Y}_{lm} \bullet W_t)^2 - (\hat{\mathbb{Y}}_{lm} \bullet W_t)^2 \\
&= B^S_{tlm} \bullet X_t + b^S_{tlm} - |S_{tlm}|^2,
\end{aligned}
$$

which is constraint (10) on apparent power.

Note that except for the rank constraint, which makes the problem non-convex, $(\mathcal{P}^{nc})$ is a convex SDP. We therefore define the problem $(\mathcal{P}^{c})$ as the convex problem, which results from removing the rank constraint from $(\mathcal{P}^{nc})$. Clearly, $(\mathcal{P}^{c})$ approximates $(\mathcal{P}^{nc})$ from below, i.e., is an *optimistic* approximation of the AC-OPF problem.

## 3. A Solution by Markovian Stochastic Dual Dynamic Programming

In this section, we will show how Markovian stochastic AC-OPF problems of type $(\mathcal{P}^{c})$ can be solved using SDDP type composition methods and discuss under which circumstances the gap between the non-convex problem $(\mathcal{P}^{nc})$ and $(\mathcal{P}^{c})$ vanishes.

In Section 3.1, we propose a dynamic programming formulation of a Markovian version of $(\mathcal{P}^{c})$ and review the concept of scenario lattices as suitable discrete approximations of randomness. Section 3.2, discusses a Markovian SDDP algorithm and provides details on how value functions

can be derived from the nodal problems on a scenario lattice. Finally, in Section 3.3, we dualize the nodal problems and show how the dual solution can be used to check for a positive duality gap in the relaxed nodal AC-OPF problems.

### 3.1. A Markovian Formulation

In this section, we will reformulate the extensive form of the stochastic programming problem in $(\mathcal{P}^c)$ to a dynamic programming formulation. For this purpose, we denote by $\xi_t$ all the random elements in the problem formulation that are measurable with respect to $\mathcal{F}_t$. Note that while potentially all data of the problem $(\mathcal{P}^c)$ may be random, in actual applications this is usually only the case for a small subset of variables.

In order to be able to obtain numerical solutions, we introduce the following running assumption.

ASSUMPTION 1 **(Finite Support)**. *The process $\xi = (\xi_1, \ldots, \xi_T)$ is finitely supported.*

REMARK 1. Note that in many instances the randomness in stochastic optimization problems is most naturally modelled as continuously distributed. In these cases, one can approximate the original stochastic process by a discrete process and then solve the problem based on the approximation. There is large literature that deals with qualitative and quantitative bounds on the error induced by this approach (e.g. Shapiro et al. 2009, Heitsch and Römisch 2009, Pflug and Pichler 2014, Kiszka and Wozabal 2020, Löhndorf and Wozabal 2021). Here, we will ignore this complication and assume that Assumption 1 is either naturally fulfilled or, alternatively, that the problem can be closely approximated by a problem based on a finitely supported process $\xi$. □

The most general representation of a discrete time and discrete value stochastic process is a scenario tree, an example of which is displayed in Figure 3 (left). However, in a scenario tree where every node has more than one successor, the number of nodes necessarily grows exponentially in the number of stages. To deal with this complication, scenario trees typically have only a few stages or contain nodes with only one successor, which effectively leads to deterministic sub-problems at these nodes.

The complexity of a scenario tree can be reduced substantially if the data process is Markovian. In this case, the conditional distributions of $\xi_{t+1}$ depend only on $\xi_t$ instead of the entire history of the process. This means that all histories $(\xi_1, \ldots, \xi_t)$ of the process that lead to the same state $\xi_t$ continue in identical sub-trees that can be combined without loss of information. In line with the terminology often used in mathematical finance, we refer to such *recombining* scenario trees as *scenario lattices*.

An example of a scenario lattice is depicted in Figure 3 (right). Formally, a scenario lattice is a graph organized in a finite number of layers. Each layer is associated with a discrete point in time

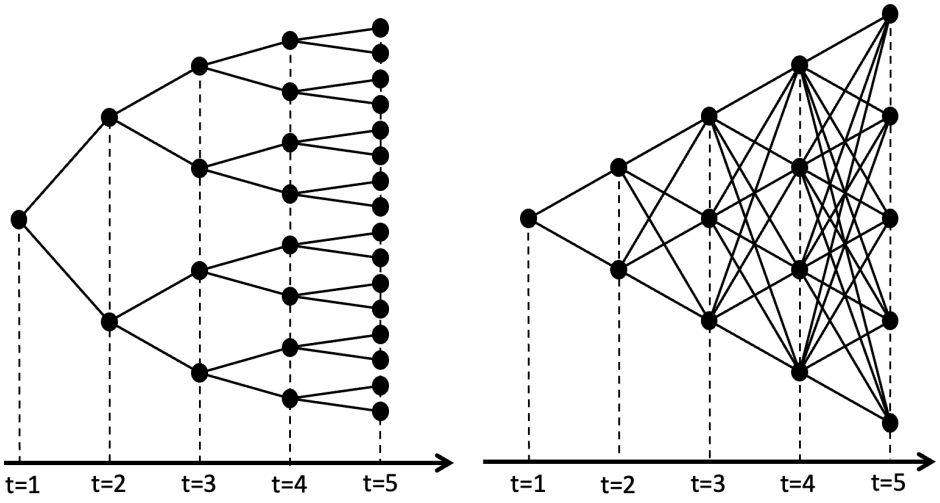


**Figure 3** A tree with 31 nodes representing 16 scenarios on the left and a lattice with 15 nodes representing 120 scenarios on the right.

and contains a finite number of nodes. Successive layers are connected by arcs. A node represents a possible state of the stochastic process and an arc indicates the possibility of a state transition between the two connected nodes. Each arc connecting node $i$ in stage $t$ with node $j$ in stage $t+1$ is associated with a probability weight $p_{tij}$ and the weights of outgoing arcs of a node add up to one. Note that this definition also covers inhomogeneous Markov processes where conditional distributions change over time. A scenario tree differs from a scenario lattice by the additional requirement that every node in $t$ has only one predecessor in $(t-1)$.

We denote the number of nodes of a scenario lattice in stage $t$ by $N_t$, and $\xi_{tj}$, $j \in [N_t]$ as the state of the lattice process at node $j$ in stage $t$. Assuming that all state transitions between nodes in consecutive stages have positive probabilities, the number of scenarios modeled by the lattice equals $\prod_{t=1}^{T} N_t$. As the number of stages grows, additional nodes needed to construct a lattice are those of the newly added stages. By contrast, the number of nodes in a scenario tree – assuming that each node has more than one successor – grows exponentially in the number of stages. We refer to Kiszka and Wozabal (2020) for a more in depth treatment of scenario lattices and their properties.

In order to use scenario lattices in stochastic programming, we additionally need the decisions in stage $t$ do not *explicitly* depend on the whole history of the problem, but only *implicitly* via the current state of the problem. To formalize this concept, we define the state of the problem at time $t$ as $\xi_t$ and $X_{t-1}$ with $\xi_t$ as the *environmental state*, which evolves randomly independent of the decisions, and $X_{t-1}$ as the *resource state*, which can be directly controlled by the decision maker. Summarizing, to avoid the exponential explosion of complexity in the number of stages, we assume

that the problem is Markovian in the stochastic process as well as in the decisions as detailed in the following assumption.

ASSUMPTION 2 **(Markovian Stochastic Programming Problem)**. 1. *The stochastic process $\xi_t$ is Markovian, i.e.,* $\mathbb{E}[\xi_{t+1}|\mathcal{F}_t] = \xi_t$.

2. *The decision $X_t$ depends on $(X_1, \ldots, X_{t-1})$ only via its dependence on $X_{t-1}$.*

We note that Assumption 2 is natural in a most situations and for the problems where this is not the case, it can in principle always be enforced by a state space expansion.

Using Assumption 2, we represent $(\mathcal{P}^c)$ by its dynamic programming equations

$$C_t(\xi_{tj}, X_{t-1}) = \begin{cases} \min\ F_t \bullet X_t + \mathbb{E}[C_{t+1}(\xi_{t+1}, X_t)|\xi_t = \xi_{tj}] \\ \text{s.t.}\ \ (X_t, W_t) \in \mathcal{X}_t(\xi_{tj}, X_{t-1}), \end{cases} \tag{14}$$

where $C_{T+1} \equiv 0$, $\mathcal{X}_t(\xi_{tj}, X_{t-1})$ is the feasible set for stage $t$, and all random elements take the values stored at lattice node $\xi_{tj}$. Note that all our results remain valid if we use any other SDP representable convex function $C_{T+1}$ as a boundary condition.

If the expected cost-to-go functions

$$(\xi_{tj}, X_t) \mapsto \mathcal{C}_{t+1}(\xi_{tj}, X_t) := \mathbb{E}[C_{t+1}(\xi_{t+1}, X_t)|\xi_t = \xi_{tj}]$$

are known explicitly, the problems in (14) reduce to deterministic AC-OPF problems that depend on the current state and relate to the next stage via $\mathcal{C}_{t+1}$, which in turn depends on the decisions taken at time $t$. Furthermore, note that the expected cost-to-go functions $\mathcal{C}_{t+1}$ depend only on $\xi_t$ and $X_t$ due to Assumption 2.

The following proposition relates the solution of the dynamic programming equations (14) with the solution of the original stochastic optimization problem.

PROPOSITION 1. *If Assumptions 1 and 2 hold and for all $t \in \mathcal{T}$, all realizations of $(\xi_1, \ldots, \xi_t)$, and all optimal solutions $X_{t-1}$ of $C_{t-1}$, there are optimal solutions $(X_t, W_t)$ such that the matrix $W_t$ has rank* 1*, then the optimal values and solutions for* (14) *are also optimal for the original problem* $(\mathcal{P}^{nc})$.

*Proof.* If $C_t(\xi_t, X_{t-1})$ has an optimal solution $(X_t, W_t)$ with $\operatorname{rank}(W_t) = 1$, then there is a voltage vector $V_t \in \mathbb{C}^n$ such that $W_t = \tilde{V}_t \tilde{V}_t^\top$. The vectors $V_t$ are thus physically feasible for the original AC-OPF problems in state $(\xi_t, X_{t-1})$. If all $(\xi_t, X_{t-1})$ have that property, the approximations of the non-convex AC-OPF problem on the nodes are tight and $(X_t, V_t)$ are the solutions of the dynamic programming equations for the original problem $(\mathcal{P}^{nc})$ and thus optimal. □

### 3.2. A Solution by Stochastic Dual Dynamic Programming

While stochastic optimization problems that use scenario trees to discretize randomness can be solved via their deterministic equivalent by assigning one decision vector to each node of the tree, this property is lost when using scenario lattices.

In particular, since the lattice does not contain the information on the history of the process, optimal decisions do not only depend on the environmental state $\xi_t$ but also on the resource state $X_{t-1}$, which is not uniquely defined for a node but depends on the history of the decision process. Hence, in order to solve the problem one has to obtain the cost functions $\mathcal{C}_t$, which effectively define the optimal policy via the optimization problems (14).

In order to obtain cost functions, we propose to use SDDP which is a sampling based decomposition algorithm that allows to learn increasingly accurate approximations of $\mathcal{C}_t$. The algorithm goes back to the seminal work of Pereira and Pinto (1991) and its Markovian version to Mo et al. (2001) and has been extensively used to solve problems in energy planning. Convergence proofs of the algorithm can be found in Philpott and Guan (2008) for linear problems and Girardeau et al. (2015) for the general convex case.

The main idea of SDDP is to approximate the cost-to-go functions $\mathcal{C}_t$ by a piecewise affine model $\bar{\mathcal{C}}_t$. This is based on the fact that since the problems (14) are convex and $X_{t-1}$ only enters the right hand sides of the constraints, the functions $\mathcal{C}_t(\xi_t, X_{t-1})$ are convex and can be approximated below by a maximum of affine functions whose slopes are the subgradients of $\mathcal{C}_t$ at finitely many trial points $X_{t-1}$.

The SDDP algorithm alternates between simulating the decision policy (forward pass) based on the current approximations $\bar{\mathcal{C}}_t$ and recursively updating the piecewise affine models $\bar{\mathcal{C}}_t$ (backward pass). In order to describe the algorithm in more detail, we define the approximated problem on lattice node $j$ in period $t$ in the $l$-th iteration as

$$\bar{C}_{tl}(\xi_{tj}, X_{t-1}) = \left\{ \begin{array}{lll} \min\ F_t \bullet X_t + \theta & & \\ \text{s.t.}\ \ \mathbb{Y}_k \bullet W_t = A^P_{tk} \bullet X_t + a^P_{tk}, & \forall k \in \mathcal{N} & [\lambda_k] \\ \quad \hat{\mathbb{Y}}_k \bullet W_t = A^Q_{tk} \bullet X_t + a^Q_{tk}, & \forall k \in \mathcal{N} & [\gamma_k] \\ \quad M_k \bullet W_t = A^V_{tk} \bullet X_t + a^V_{tk}, & \forall k \in \mathcal{N} & [\mu_k] \\ \quad \mathbb{Y}_{lm} \bullet W_t \le B^P_{tlm} \bullet X_t + b^P_{tlm}, & \forall (l,m) \in \mathcal{L} & [\lambda_{lm}] \\ \quad \begin{bmatrix} -B^S_{tlm} \bullet X_t - b^S_{tlm} & \mathbb{Y}_{lm} \bullet W_t & \hat{\mathbb{Y}}_{lm} \bullet W_t \\ \mathbb{Y}_{lm} \bullet W_t & -1 & 0 \\ \hat{\mathbb{Y}}_{lm} \bullet W_t & 0 & -1 \end{bmatrix} \preceq 0, & \forall (l,m) \in \mathcal{L} & [r_{lm}] \\ \quad M_{lm} \bullet W_t \le B^V_{tlm} \bullet X_t + b^V_{tlm}, & \forall (l,m) \in \mathcal{L} & [\mu_{lm}] \\ \quad A^1_{ti} \bullet Z_{t-1} + A^2_{ti} \bullet X_t \le a_{ti}, & \forall i \in [s_t] & [\sigma_i] \\ \quad Z_{t-1} = X_{t-1}, & & [\Phi] \\ \quad e_{ti} + E_{ti} \bullet X_t \le \theta, & \forall i \in [l-1] & [\nu_i] \\ \quad X_t \succeq 0,\ W_t \succeq 0, & & \end{array} \right.$$

**Algorithm 1** Markov Chain SDDP

**Require:** Lattice $\xi$, number of iterations L, start state $X_0$

1: $l \leftarrow 1$ {initialize}
2: **while** $l \leq L$ **do** {main loop}
3: $\hat{\xi}_1^l \leftarrow \xi_1$, $\hat{X}_0^l = X_0$
4: **for** $t \in [T]$ **do** {forward pass}
5: Get solutions $\hat{X}_t^l$ for $\bar{C}_{tl}(\hat{\xi}_t^l, \hat{X}_{t-1}^l)$
6: Sample $\hat{\xi}_{t+1}^l$ given $\hat{\xi}_t^l$ from $\xi_t$
7: **end for**
8: **for** $t \in T : 2$ **do** {backward pass}
9: **for** $j \in [N_t]$ **do**
10: Get objective $o_{tlj}$ and dual $\Phi_{tlj}$ for $\bar{C}_t(\xi_{tj}, \hat{X}_{t-1}^l)$
11: **end for**
12: **for** $i \in [N_{t-1}]$ **do** {generate new cuts}
13: $e_{t-1,il} \leftarrow \sum_{j\in[N_t]} p_{t-1,ij} o_{tlj}$, $E_{t-1,il} \leftarrow \sum_{j\in[N_t]} p_{t-1,ij} \Phi_{tlj}$
14: **end for**
15: **end for**
16: $l \leftarrow l + 1$
17: **end while**

where the decision variables are $X_t$, $W_t$ and $Z_{t-1}$, the dual multipliers of the constraints are indicated in square brackets, and realizations for random data are taken from node $\xi_{tj}$.

Note that $\theta$ together with the second last constraint models the piecewise affine approximation of the value function at lattice node $j$ that has been constructed in the first $(l-1)$ iterations. Also note that $Z_{t-1}$ is introduced purely for notational convenience to extract a subgradient of the function $X_{t-1} \mapsto \bar{C}_{tl}(\xi_{tj}, X_{t-1})$ as the dual multiplier $\Phi$ of the constraint $Z_{t-1} = X_{t-1}$.

In our general formulation the resource state of the problem consists of all the decisions in $X_t$, which is typically not required – see for example the application in Section 4, where only a small fraction of $X_t$ is relevant for the decision on the next stage. However, in order simplify the exposition, we do not explicitly distinguish between environmental state variables and decisions that are taken in period $t$.

We summarize SDDP in Algorithm 1 defining $L$ as the number of iterations. The algorithm takes a scenario lattice $\xi$ and a start state $X_0$ as inputs. In the forward passes (lines 4 to 6) the algorithm simulates a path from the lattice process and solves the problems $\bar{C}_{tl}$ at the sampled lattice nodes using the value function approximations trained so far. In the backward pass (lines

8 to 14), the algorithm solves the problems on all the nodes at the resource states sampled in the forward pass and extracts an affine cut that is added to the representation of the respective value functions at the nodes of the lattice one stage earlier by multiplying with the corresponding conditional probabilities in line 13.

Note that we do not incorporate a convergence check but stop after a predetermined number of $L$ iterations. Alternatively, one can periodically estimate the optimality gap

$$\text{gap}_l = U_l - \bar{C}_{1l}(\xi_1, X_0),$$

where

$$U_l = \mathbb{E}\left[\sum_{t=1}^{T} F_t \bullet X_{tl}\right]$$

is the expected value of the policy $X_{tl}$ that results from solving the nodal problems using the value functions approximations $\bar{C}_{tl}$ to represent future costs. Note that the cost functions approximation $\bar{C}_{1l}$ is a lower bound for the convex relaxation of the AC-OPF problem and therefore also for the original non-convex problem. On the other hand, $U_l$ is an upper bound of the optimal value for the relaxed problem because the decisions $X_{tl}$ are based on approximations of the real value functions and the resulting policies are therefore suboptimal. Hence, for any iteration $l$, $\text{gap}_l$ is an upper bound on the optimality gap of the SDDP policy for the relaxed AC-OPF problem.

In order to obtain an estimate of this gap, one can sample $U_l$ by computing $K$ forward passes based on independent samples $(\hat{\xi}_t^k)_{k\in[K],t\in\mathcal{T}}$ from the lattice and recording their objective values, i.e.,

$$\hat{U}_l^K = K^{-1}\sum_{k=1}^{K}\sum_{t=1}^{T} \hat{F}_t^k \bullet \hat{X}_t^k,$$

where $\hat{X}_t^k$ is the sampled decision and $\hat{F}_t^k$ is the objective value coefficient which belongs to the sampled node $\hat{\xi}_t^k$. An unbiased estimate of the gap is therefore

$$\widehat{\text{gap}}_l^K = \hat{U}_l^K - \bar{C}_{1l}(\xi_1, X_0).$$

Note that $\widehat{\text{gap}}_l^K$ is a random quantity, since it is based on a sampled upper bound $\hat{U}_l^K$. See Shapiro (2011) for a discussion on how to use confidence bands around $U_l^k$ in convergence checks. Further note that $\widehat{\text{gap}}_l^K$ is potentially underestimating the gap between the SDDP policy and the costs of the *true* non-convex AC-OPF problem, since $\hat{U}_K^l$ might be smaller than the cost of the non-convex AC-OPF problem.

Our discussion of the convergence properties is based on Girardeau et al. (2015), who show that SDDP converges almost surely to the true solution of the problem if the problem is convex, the feasible set of decisions is compact, and the problems have relatively complete recourse. We therefore make the following assumption.

ASSUMPTION 3. *($\mathcal{P}^{nc}$) has relatively complete recourse and a compact feasible set.*

Based on this, we summarize the convergence results for SDDP in the following proposition.

PROPOSITION 2. *For a problem ($\mathcal{P}^{nc}$) fulfilling Assumptions 1 – 3, the following holds:*

1. *The cost function approximation for the first stage $\bar{C}_{1l}(\xi_1, X_0)$ is a valid lower bound for the objective value of the multi-stage stochastic AC-OPF problem ($\mathcal{P}^{c}$) and therefore also for ($\mathcal{P}^{nc}$).*
2. *As $L \to \infty$, Algorithm 1 converges, i.e., $\widehat{gap}_l^K \to 0$ and the optimal solutions obtained using the cost functions approximations $\bar{\mathcal{C}}_t$ converge to the optimal solutions of ($\mathcal{P}^{c}$).*
3. *For any given $l$, if the problems in the $K$ forward passes defining $\hat{U}_l^K$ yield physically feasible solutions for the non-convex problems on the nodes, then $\widehat{gap}_l^K$ is an unbiased estimate of an upper bound on the gap between the SDDP policy and the true objective of ($\mathcal{P}^{nc}$).*
4. *If there is a $\bar{l}$ such that for all $l \geq \bar{l}$ all nodal problems in forward and backward passes yield physically implementable solutions, then the optimal objective values calculated by Algorithm 1 converge to the true value of ($\mathcal{P}^{nc}$).*

*Proof.* The first three points follow from Proposition 1 and Girardeau et al. (2015).

To see the last point, we define $C_t^{nc}$ as the cost function of the non-convex problem and note that due to our assumption $C_T(X_{T-1}, \xi_{Tj}) = C_T^{nc}(X_{T-1}, \xi_{Tj})$ for all optimal decisions $X_{T-1}$ and all lattice nodes $\xi_{Tj}$, which establishes that $\mathcal{C}_T = \mathcal{C}_T^{nc}$ at all lattice nodes and all points chosen by the optimal policy.

In the second last stage, we note that due to 2, we have

$$F_{T-1} \bullet X_{T-1,L} + \bar{\mathcal{C}}_{TL}(X_{T-1,L}, \xi_{T-1,j}) \xrightarrow{L\to\infty} F_{T-1} \bullet X_{T-1} + \mathcal{C}_T(X_{T-1}, \xi_{T-1,j})$$

where $X_{T-1,L}$ and $X_{T-1}$ are the optimal decisions for the problem with value functions $\bar{\mathcal{C}}_{TL}$ and $\mathcal{C}_T$ respectively. At the same time, due to the above and our assumption that

$$F_{T-1} \bullet X_{T-1,L}^{nc} + \bar{\mathcal{C}}_{TL}(X_{T-1,L}^{nc}, \xi_{T-1,j}) = F_{T-1} \bullet X_{T-1,L} + \bar{\mathcal{C}}_{TL}(X_{T-1,L}, \xi_{T-1,j})$$

where $X_{T-1,L}^{nc}$ is the optimal decision for the non-convex problem at lattice node $\xi_{T-1,j}$ and some resource state $X_{T-2}$, we have $\mathcal{C}_{T-1} = \mathcal{C}_{T-1}^{nc}$. Continuing in this manner until the first stage establishes 4. □

Point 3 of Proposition 2 establishes that even if the convex relaxations of the AC-OPF problems in the nodes are not tight, one could use a computationally more expensive method to ensure physically feasible solutions to solve problems $\bar{C}_{tL}$ in the forward pass to make sure that $\widehat{\text{gap}}_l^K$ is a valid estimate of the optimality gap for the non-convex problem. In the next section, we will discuss this point in more detail and propose a method how to obtain such a physically feasible policy by modifying the forward simulations in convergence checks.

### 3.3. Dualization of Nodal Problems and Reconstruction of Voltages

Following Lavaei and Low (2012), we solve the dual of the nodal problems to compute $\bar{C}_{tl}$ in Algorithm 1 instead of the primal as this allows to check whether the relaxation of the original non-convex problem on the nodes is tight. In particular, the solutions $W_t$ of the primal problem usually do not have rank 1, even if there is an optimal rank 1 solution. Luckily, in most cases the dual solution of $\bar{C}_{tl}$ allows for the construction of a voltage vector that is part of an optimal solution of the original non-convex primal problem.

For the dual approach to work, we have to ensure that there is no duality gap between primal and dual nodal problems. Unlike in linear programming, for SDPs a Slater condition has to be fulfilled to show strong duality. Unfortunately, it is not possible to verify this condition for problem $\bar{C}_{tl}$ in general. However, as is shown in Section 4, the constraints related to power flow are generally unproblematic in this regard and in particular allow for inner points of the feasible sets. At this point we therefore make the following abstract assumption, which ensures strong duality between the primal and dual problems.

ASSUMPTION 4 **(Slater's Condition)**. *The problems $\bar{C}_{tl}$ have finite optimal value and the feasible sets of the dual problem have an interior point.*

In order to dualize, we write out the Lagragian of $\bar{C}_{tl}(\xi_{tj}, X_{t-1})$. To that end, we denote the elements of the symmetric matrix $r_{lm}$ by

$$r_{lm} = \begin{pmatrix} r^1_{lm} & r^2_{lm} & r^3_{lm} \\ r^2_{lm} & r^4_{lm} & 0 \\ r^3_{lm} & 0 & r^5_{lm} \end{pmatrix}$$

and define the following functions of the collection of dual variables denoted by $\alpha$

$$\begin{aligned}
h_t(\alpha) &= \sum_{k\in\mathcal{N}} \left(-\lambda_k a^P_k - \gamma_k a^Q_k - \mu_k a^V_k\right) - \sum_{(l,m)\in\mathcal{L}} \left(\lambda_{lm} b^P_{lm} + r^1_{lm} b^S_{lm} + r^4_{lm} + r^5_{lm} + \mu_{lm} b^V_{lm}\right) \\
&\quad - \sum_{i\in[s_t]} \sigma_i a_i + \Phi X_{t-1} + \sum_{i\in[l]} \nu_i e_{tnl} \\
G_t(\alpha) &= \sum_{k\in\mathcal{N}} \lambda_k \mathbb{Y}_k + \gamma_k \hat{\mathbb{Y}}_k + \mu_k M_k \\
&\quad + \sum_{(l,m)\in\mathcal{L}} \left(\lambda_{lm} \mathbb{Y}_{lm} + 2r^2_{lm} \mathbb{Y}_{lm} + 2r^3_{lm} \hat{\mathbb{Y}}_{lm} + \mu_{lm} M_{lm}\right) \\
H_t(\alpha) &= F_t - \sum_{k\in\mathcal{N}} \left(\lambda_k A^P_k + \gamma_k A^Q_k + \mu_k A^V_k\right) - \sum_{(l,m)\in\mathcal{L}} \left(\lambda_{lm} B^P_{lm} + r^1_{lm} B^S_{lm} + \mu_{lm} B^V_{lm}\right) \\
&\quad + \sum_{i\in[s_t]} \sigma_i A^2_{ti} + \sum_{i\in[l]} \nu_i E_{tnl}.
\end{aligned}$$

With the help of these functions, we can write the Lagrangian as

$$\mathcal{L}(W_t, X_t, Z_t, \theta, \alpha) = h_t(\alpha) + G_t(\alpha) \bullet W_t + H_t(\alpha) \bullet X_t + Z_{t-1} \bullet (-\Phi + A^1_{ti}\sigma_i) + \theta \left(1 - \sum_{i\in[l]} \nu_i\right)$$

which by minimax duality leads to the following dual problems on the nodes

$$\bar{C}_{tl}(X_{t-1},\xi_{tj}) = \begin{cases} \max\limits_{\alpha} \ \mathbb{E}\left[h(\alpha)\right] \\ \text{s.t.} \quad G_t(\alpha) \succeq 0,\ H_t(\alpha) \succeq 0 \\ \qquad r_{lm} \succeq 0, \quad \forall (l,m) \in \mathcal{L} \\ \qquad \sum_{i\in[l]} \nu_i = 1 \\ \qquad \Phi = A^1_{ti}\sigma_i, \quad \forall i \in [s_t], \end{cases} \tag{15}$$

where the first and second inequalities are enforced by the fact that the primal variables $W_t$ and $X_t$ are symmetric and positive semi-definite.

Note that (15) is also the dual problem of the non-convex formulation of the AC-OPF problem on the lattice nodes, which include the rank condition on $W_t$ (Lavaei and Low 2012). This implies that $\bar{C}_{tl}$ is the bidual of the original non-convex AC-OPF problem on the node and consequently the tightest convex approximation. Hence, if there is no duality gap between (15) and the non-convex problem, the approximation is exact.

The advantage of the dual formulation above is that it easy to identify sufficient conditions that ensure zero duality gap in the AC-OPF problems and allow to construct a physically feasible voltage vector. We summarize these results in the following proposition, whose proof is relegated to Appendix A.2.

Proposition 3 **(Lavaei and Low (2012))**. *Let $\alpha$ and $W_t$ be optimal dual and primal solutions of problem $\bar{C}_{tl}(\bar{\xi}_{tn}, X_{t-1})$. If*

$$\dim(\ker(G_t(\alpha))) = \dim(\{x \in \mathbb{R}^{2n} : G_t(\alpha)x = 0\}) \leq 2, \tag{16}$$

*then*

1. *the problem $\bar{C}_{tl}(\xi_{tj}, X_{t-1})$ has a rank one optimal solution $W_t^\star$ implying that AC-OPF problem is solved without duality gap;*
2. *a physically feasible voltage vector $V_t^\star$ can be constructed from an arbitrary vector $\mathcal{K} = (\mathcal{K}_1, \mathcal{K}_2)^\top$ in the null space of $G_t$ and conditions on real or imaginary parts of voltages on two busses.*

Remark 2. For the second point, note that, for some $g_1$ and $g_2 \in \mathbb{R}$, we can write

$$\tilde{V}_t^\star = g_1\mathcal{K} + g_2\mathcal{K}_\perp$$

where $\mathcal{K}_\perp = (-\mathcal{K}_2^\top, \mathcal{K}_1^\top)^\top$ (see Appendix A.2). To determine $g_1$ and $g_2$, we need two conditions. As a first condition, we can use that the voltage angle at the swing bus $n_0$ equals 0 by convention, i.e.,

$$0 = g_1\mathcal{K}_{2,n_0} + g_2\mathcal{K}_{1,n_0} \Leftrightarrow g_1 = -g_2\frac{\mathcal{K}_{1,n_0}}{\mathcal{K}_{2,n_0}}.$$

As a second condition, we can use any binding voltage, power, or current constraint on a bus $\bar{m}$. We proceed for the case of a binding upper bound on the squared absolute value of voltage and remark that formulas for the other cases can be derived analogously.

Assuming $|V^{\star}_{t,\bar{m}}|^2 = \bar{V}^2_{\bar{m}}$, where $\bar{V}_{\bar{m}}$ is the upper bound on absolute value of voltage on node $\bar{m}$, yields

$$|\bar{V}_{\bar{m}}|^2 = (g_1 \mathcal{K}_{1\bar{m}} - g_2 \mathcal{K}_{2\bar{m}})^2 + (g_1 \mathcal{K}_{2\bar{m}} + g_2 \mathcal{K}_{1\bar{m}})^2$$

Substitution for $g_1$ and solving for $g_2$ results in

$$g_2 = \bar{V}_{\bar{m}} \left( \left( \frac{\mathcal{K}^2_{1,n_0}}{\mathcal{K}^2_{2,n_0}} + 1 \right) \left( \mathcal{K}^2_{1\bar{m}} + \mathcal{K}^2_{2\bar{m}} \right) \right)^{-1/2}.$$

If condition (16) is not fulfilled, then the AC-OPF problem might not be solvable efficiently. Lavaei and Low (2012) show in numerical experiments that the duality gap for a specific quadratic cost minimization problem is zero for a large number of test systems. They conclude that most real-life AC-OPF problems can be solved in polynomial time.

In our numerical case study in Section 4, we find that condition (16) is fulfilled in most problems solved in the forward and backward pass of the SDDP algorithm. However, the condition is somewhat hard to check numerically, since the eigenvalues are never exactly zero due to finite floating point precision and the implementation of interior point solvers for SDPs. One option to deal with these issues is to set numerical thresholds for considering eigenvalues to be zero as is done for example in Molzahn et al. (2013).

We propose a different approach to ensure that the solution of the dual of the relaxed OPF problem yields a physically feasible voltage vector and to construct a valid optimality gap between the SDDP policy and an optimal solution of ($\mathcal{P}^{nc}$). To this end, we first solve the equations in Remark 2 for all the binding constraints and check if there is a $\tilde{V}^{\star}_t$, which yields voltages that do not violate any voltage bounds and, up to a certain accuracy, yield the same powers on the nodes as computed with the dual solution. If this is the case, we conclude that there is a physically feasible voltage vector that reproduces the solution of the dual problem.

If on the other hand we get a difference in powers or violations of voltage bounds on the busses for all voltage vectors obtained from bindings constraints, we infer that there is a duality gap between the real problem and its convex SDP relaxation. In this case, we find a physically feasible voltage vector that reproduces the powers on the busses as close as possible by solving the non-convex problem

$$\begin{aligned} \min_{V_t} \quad & ||\mathfrak{Re}(V_t \circ Y^* V_t^*) - P_t||^{\chi}_{\chi} + ||\mathfrak{Im}(V_t \circ Y^* V_t^*) - Q_t||^{\chi}_{\chi} \\ \text{s.t.} \quad & \underline{V}^2 \leq |V_t|^2 \leq \bar{V}^2, \end{aligned} \tag{17}$$

where $\chi \geq 1$ and $P_t$ and $Q_t$ are the vectors of active and reactive powers implicitly used by the dual solution with $P_{tn} = \mathbb{Y}_n \bullet W_t$ and $Q_{tn} = \hat{\mathbb{Y}}_n \bullet W_t$ .

While the above problem is non-convex, it has only few variables and can be solved quickly with standard software. Furthermore, the computations have to be only performed in those forward passes that are used for convergence checks, i.e., in relatively few problems. In our numerical experiments, we choose $\chi > 1$ to make the objective function differentiable and aid gradient based solvers (see Section 4).

We then recalculate the cost by re-solving the primal problems $\bar{C}_{tl}$ with fixed $\hat{W}_t = \hat{V}_t \hat{V}_t^\top$, where $\hat{V}_t$ is the optimal solution of (17). Fixing $\hat{W}_t$ yields a convex SDP that is always feasible due to Assumption 3 and necessarily yields an objective value larger than $\bar{C}_{tl}$. In this way, we obtain a physically feasible decision policy and thus an unbiased upper bound $\hat{U}_L^K$ for the true optimal cost in the calculation of $\widehat{\text{gap}}_L^K$, which therefore is a valid estimate of the optimality gap of the SDDP policy relative to $(\mathcal{P}^{nc})$.

## 4. A Problem of Storage Sitting, Sizing, and Operation

In this section, we present a numerical example demonstrating the performance of the proposed framework for a medium-sized problem of sitting, sizing, and operation for grid-level battery storage systems using the IEEE RTS-GMLC network (Barrows et al. 2020) with random electricity demand and random renewable generation.

Electricity storage is a key technology that enables the integration of renewable power generation capacity by complementing random production of wind and solar plants with the flexibility to store electricity and to temporally align supply and demand avoiding blackouts as well as the overloading of lines and transformers at times of high production.

The extant literature on choosing optimal location for electric storage (sitting), determining its optimal size, and finding optimal operational decisions is extensive and we refer to Zidar et al. (2016) and Miletić et al. (2020) for a comprehensive survey.

Most authors use deterministic planning and employ either DC approximations to model power flow (e.g., Wogrin and Gayme 2015) or rely on SDP or SOCP relaxations (e.g., Gayme and Topcu 2013, Marley et al. 2017, Zafar et al. 2020).

Since electricity storage helps to deal with uncertainty of renewable production, deterministic approaches tend to underinvest in storage and arrive at solutions that perform suboptimally in practice. Therefore many authors seek to explicitly incorporate uncertainty into storage planning models. The approaches can be roughly divided into robust optimization (e.g., Jabr et al. 2015, Chowdhury et al. 2020) and stochastic optimization.

Most papers in the stochastic optimization literature employ two-stage models where the first stage represents investment decisions while the second stage models operational decisions (e.g., Oh 2011, Nick et al. 2014, Bucciarelli et al. 2018). Some authors use this setup combined with chance constraints to limit the probability of network failure (e.g., Kargarian et al. 2016, Baker et al. 2017, Reddy 2017).

There are only few authors that use multi-stage stochastic programming and explicitly model the uncertainty in storage operation over several time stages when deciding on storage capacity. Pandzic et al. (2015), Qiu et al. (2017) employ a three stage model using DC power flow while to the best of our knowledge Xiong and Singh (2016) is the only truly multi-stage approach using scenario trees. However, the authors use a DC approximation and a rather crude modeling of randomness using a trinomial scenario tree.

In the following, we propose what we believe is the first stochastic optimization model that combines the decision about storage investment on the first stage with multiple daily stages of stochastic planning in hourly resolution representing the operation of the power system. In Section 4.1, we describe our modeling of the stochastic processes for demand, wind power generation, and solar power. In Section 4.2, we describe the optimization model as an instance of the general model class described in Section 3, while Section 4.3 is dedicated to the discussion of our numerical results.

### 4.1. Stochastic Processes

We use the IEEE RTS-GMLC network (Barrows et al. 2020) that contains 74 busses partitioned in three areas and is one of the few publicly available test cases that, next to technical specifications of the grid and power generation, also contains one year of data on demand as well as renewable generation on the busses for the year 2020.[1] For our numerical experiments, we only use the 24 busses in area 1 of the network.

We model conventional demand, wind power production, as well as photovoltaic production as random. For each of these variables we use hourly data on day-ahead forecasts to estimate a 24-dimensional aggregate stochastic process in daily resolution for the whole network. Since there is only one bus in area 1 that has installed wind power capacities, we directly model wind power production at this bus. To disaggregate load and PV power production to single busses, we apply fixed scaling factors. More specifically, for load we apply the scaling factors given in the case description to arrive at bus-level active and reactive power demands, while for PV production, we model cumulative production at all busses and then disaggregate to individual busses proportional to yearly production volumes.

[1] All case related data is available at `https://github.com/GridMod/RTS-GMLC`.

This implies that we model a $3 \times 24 = 72$ dimensional stochastic process that evolves in daily time increments. In order to model the process, we first capture the variation that can be attributed to seasonal effects and then reduce the dimensionality of the process using principal component analysis (PCA).

To this end, for each of the three random processes, we set up a linear regression model with a constant term, 23 dummies for the hours of the day, a weekend dummy, and yearly seasonality modeled by the two regressors $\cos\left(2\pi d/366\right)$, $\sin\left(2\pi d/366\right)$, which together represent a yearly sinusoidal pattern with a variable amplitude and phase shift dependent on the day $d \in [366]$ of the year. We then use all quadratic interactions of these regressors and end up with 299 regressors in each of the models. To avoid overfitting, we estimate the model with LASSO regression where the degree of regularization is chosen by 10-fold cross validation.

While the fit of the model for PV production and load is rather good with a $R^2$ of 93% and 96.3% respectively, the fit for wind power production is, as expected, considerably worse with an $R^2$ of 23.4%, since wind speeds do not follow a clear seasonal pattern.

We base our stochastic model on the residuals $u_{dhj}$ on day $d$, in hour $h$ for variable $j = 1, 2, 3$ of the regression models. To deal with the pronounced heteroskedasticity of the residuals, we employ quantile transformations, i.e., we transform $\kappa_{djh} = F_{jh}^{-1}(u_{dhj})$, where $F_{jh}^{-1}$ is the inverse empirical distribution of all the residuals of variable $j$ in hour $h$. In this way the residuals are uniformly distributed on $[0, 1]$ for every hour $h$ and variable $j$.

Finally, for every day $d$, we end up with a vector of residuals $\kappa_d \in \mathbb{R}^{72}$, which collects the transformed errors for all three technologies for the 24 hours of the day. To reduce the dimensionality of this process, we perform a PCA on the 366 vectors $\kappa_d$ associated with the one year of data provided with the case and model the first 6 principle components $\Lambda_1, \ldots, \Lambda_6$, which together account for more than 95% of the variance as basic stochastic factors in our model. To capture the day by day autocorrelation structure of the components, we use LASSO regression with 10-fold cross validation to estimate a six dimensional vector autogressive model

$$\Lambda_d = \mathfrak{L}\Lambda_d + \tau_d, \tag{18}$$

where $\mathfrak{L}$ is the lag operator.

To simulate from our stochastic process, we resample the residuals $\tau_d \in \mathbb{R}^6$ of the regression model (18) to generate scenarios $\hat{\Lambda}_d$. These scenario are in turn transformed to residuals $\hat{\kappa}_d \in \mathbb{R}^{72}$ by mulitplying with the first 6 rows of the coefficient matrix of the PCA which is further transformed to $\hat{u}_d$ with linearly interpolated versions of $F_{jh}$.

Finally, the seasonal linear models are used to predict seasonal means for wind and solar production as well as load to which the corresponding simulated residuals $\hat{u}_d$ are added to arrive at

scenarios for the three variables of interest. We use the resulting scenarios to generate a scenario lattice using the stochastic gradient descent method described in Löhndorf and Wozabal (2021).

For our optimization models we are interested in residual demand for active and reactive power $P^D_{dhk}$ and $Q^D_{dhk}$ on day $d$, hour $h$ and on bus $k$, which we calculate by subtracting the renewable production at bus $k$ from the load.

### 4.2. Optimization Problem

We consider a stochastic optimization problem with 8 stages $\mathcal{D} = \{0, \dots, 7\}$: in the first stage $d = 0$, the investment decision on storage capacity is taken and the remaining 7 stages represent one week of operational planning, for which, following Barrows et al. (2020), we choose the $10^{\text{th}}$ to the $16^{\text{th}}$ of July. On every of the days $d \in [7]$, we plan for the hours $\mathcal{H} = \{1, \dots, 24\}$ in hourly resolution, i.e., we solve 24 AC-OPF problems per stage instead of one as in the models in Section 3. The overall problem setup largely follows Barrows et al. (2020) and Helistö et al. (2019) and additionally relaxes unit commitment constraints enabling a fully convex modeling of conventional dispatchable power plants.

We note that in order to get an accurate picture of the value of storage, one would have to include days from all seasons. Strategies for doing so are for example discussed in Qiu et al. (2017) or Xiong and Singh (2016). Since we are mainly interested in the performance of SDDP for AC-OPF problems, we abstain from these complications in the present paper.

In order to make the investment in electricity storage more attractive, we change the energy mix towards a future partially decarbonized system. To that end, we phase out the coal plants at nodes 101, 102, 115, 116, and 123 with capacities 76MW, 76MW, 155MW, 155MW, and 350MW respectively, jointly accounting for 73% of coal generation capacity. To compensate for the loss of fossil production, we double renewable capacities by multiplying the simulated production by 2.

We denote by $\mathcal{G} = \{1, 2, \dots, m\}$ the set of all generators and by $\mathcal{G}_k \subseteq \mathcal{G}$ the set of generators at bus $k$. Furthermore, we let $\mathcal{N}^S \subseteq \mathcal{N}$ be the subset of buses where a storage can be built and choose $\mathcal{N}^S$ to be equal to the eight buses with renewable production capacities. We denote the first-stage decision on energy capacity (in MWh) by $\bar{B}_k$ for $k \in \mathcal{N}^S$.

In line with the phase-out of much of fossil fuel capacities and the ramp-up of renewables, we assume a 2030 scenario for storage cost and use the projections of Cole and Frazier (2020) who estimate a cost of 208$/kWh for grid-level battery storage. Due to lack of detailed cost estimates as functions of energy and power capacity, we follow Cole and Frazier (2020) in assuming that the *duration* of the storages is four hours, i.e., that the storage runs empty latest within four hours if it is discharged at full power capacity. Correspondingly, the maximum real power charge and

discharge are $\eta^{-1}\bar{B}_k/4$, $\eta\bar{B}_k/4$, where $\eta \in (0,1)$ is the efficiency of the storage, which for the sake of simplicity is assumed to be symmetric for charging and discharging.

To scale down cost to one week of planning, we compute annuities based on a life time of 20 years and an interest rate of 2% yielding a weekly investment cost of $f^B = 230\$/\text{MWh}$, where we assume for the sake of simplicity that the year has exactly 52 weeks.

This leads to the following first-stage problem, in the $l$-th iteration of the SDDP algorithm

$$\bar{C}_{0l}(\xi_0) = \begin{cases} \min\ f^B \sum\limits_{k\in\mathcal{N}^S} \overline{B}_k + \theta \\ \text{s.t.}\ \ e^0_{0i} + \overline{B}^\top e^1_{0i} \le \theta, \quad \forall i \in [l-1], \end{cases}$$

where $\overline{B} = (\overline{B}_k)_{k\in\mathcal{N}^S} \in \mathbb{R}^{|\mathcal{N}^S|}$ and $e^0_{0i}$ and $e^1_{0i}$ are the intercepts and slopes of the affine functions that approximate $\mathcal{C}^1$.

Next, we describe the operational problems $\bar{C}_{dl}$ in stages $d \in [7]$, which are solved in the forward and backward passes of SDDP *on the nodes of the lattice*. We therefore assume that the random residual demands are read from the corresponding lattice node and drop the time index $d$ of the day to keep the notation manageable.

To operate the storage, we decide about real injections and withdrawals $O^+_{hk} \ge 0$, $O^-_{hk} \ge 0$, which are subject to the constraints

$$O^+_{hk} \le \frac{\overline{B}_k}{4\eta}, \quad k \in \mathcal{N}^S, \forall h \in \mathcal{H} \quad [\overline{\beta}^+_{hk}] \tag{19}$$

$$O^-_{hk} \le \frac{\eta\overline{B}_k}{4}, \quad k \in \mathcal{N}^S, \forall h \in \mathcal{H} \quad [\overline{\beta}^-_{hk}] \tag{20}$$

and the storage balance constraints for the storage level $B_{hk}$

$$B_{hk} = B_{h-1,k} + \eta O^+_{hk} - \eta^{-1} O^-_{hk}, \qquad \forall k \in \mathcal{N}^S, \forall h \in \mathcal{H} \quad [\sigma_{hk}] \tag{21}$$

$$B_{hk} \le \overline{B}_k, \qquad \forall k \in \mathcal{N}^S, \forall h \in \mathcal{H} \quad [\overline{\kappa}_{hk}], \tag{22}$$

where the initial storage level $B_{0k}$ is the level in hour $h = 24$ on the previous day and together with the storage capacities $\bar{B}_k$ form the environmental state. Note that the Greek letters in the square brackets are the dual variables of the respective constraints.

Since we start planning on a Monday after the weekend which is characterized by low loads, we assume the storage to be 75% filled in the first hour of stage 1.[2] In order to avoid end-of-horizon effects we force the storage back to its initial level, by imposing the following constraints in the last hour of the problem in $d = 7$,

$$B_{24,k} = 0.75 \times \bar{B}_k, \quad \forall k \in \mathcal{N}^S, \quad [\delta_k]. \tag{23}$$

[2] Alternatively, one could make the initial storage level a decision variable converting the problem to an infinite horizon logic.

Apart from electricity storage power can be provided by generators. As specified in the case description, we assume the cost of power generation $f^g$ to be a convex, piecewise linear function of active power generation $P^G_{tg}$ with break points $(a_{gi}, b_{gi})$ $i = 1, \dots, r_g$ such that

$$f^g(P^G_{hg}) = \begin{cases} m_{g1}(P^G_{hg} - a_{g1}) + b_{g1}, & a_{g1} < P^G_{hg} \leq a_{g2} \\ m_{g2}(P^G_{hg} - a_{g2}) + b_{g2}, & a_{g2} < P^G_{hg} \leq a_{g3} \\ \vdots & \vdots \\ m_{g(r_g-1)}(P^G_{hg} - a_{g(r_g-1)}) + b_{g(r_g-1)}, & a_{g(r_g-1)} < P^G_{hg} \leq a_{gr_g}. \end{cases}$$

To keep the problem convex, we relax the on/off constraints of the power plants, set the lower bound on production $\underline{P}_g = a_{g,1} = 0$, and impose the following linear constraints on active and reactive power generation in hour $h$

$$P^G_{hg} \leq \overline{P}_g, \qquad \forall g \in \mathcal{G}, \forall h \in \mathcal{H} \quad [\overline{\lambda}_{hg}] \tag{24}$$

$$\underline{Q}_g \leq Q^G_{hg} \leq \overline{Q}_g, \qquad \forall g \in \mathcal{G}, \forall h \in \mathcal{H} \quad [\underline{\gamma}_{hg}, \overline{\gamma}_{hg}]. \tag{25}$$

We denote by $P^D_{hk}$ and $Q^D_{hk}$ the active and reactive power demand in hour $h$ at node $k$, which is the difference of conventional demand and renewable generation

$$P_{hk} = \mathbb{Y}_k \bullet W_h = \sum_{g \in \mathcal{G}_k} P^G_{hg} - P^D_{hk} - O^+_{hk} + O^-_{hk} + D^{P+}_{hk} - D^{P-}_{hk}, \qquad \forall k \in \mathcal{N}, \forall h \in \mathcal{H} \quad [\lambda_{hk}] \tag{26}$$

$$Q_{hk} = \hat{\mathbb{Y}}_k \bullet W_h = \sum_{g \in \mathcal{G}_k} Q^G_{hg} - Q^D_{hk} + D^{Q+}_{hk} - D^{Q-}_{hk}, \qquad \forall k \in \mathcal{N}, \forall h \in \mathcal{H} \quad [\gamma_{hk}], \tag{27}$$

where $D^+_{hk}$ and $D^-_{hk}$ are curtailment of demand and supply with associated cost $f^{D+}$ and $f^{D-}$, which we set to 1000\$/MWh and 100\$/MWh, respectively. This implies that renewable production can be curtailed for a moderate fee, while it is considerably more expensive to curtail load. Note that the possibility of curtailment ensures that the problems at the nodes are always feasible and that Assumption 3 is fulfilled.

Furthermore, we impose the following constraints on voltages and powers

$$(\underline{V}_k)^2 \leq |V_{hk}|^2 = M_k \bullet W_h \leq (\overline{V}_k)^2, \qquad \forall k \in \mathcal{N}, \forall h \in \mathcal{H} \quad [\underline{\mu}_{tk}, \overline{\mu}_{tk}] \tag{28}$$

$$|S_{hlm}|^2 = (\mathbb{Y}_{lm} \bullet W_h)^2 + (\hat{\mathbb{Y}}_{lm} \bullet W_h)^2 \leq \overline{S}^2_{lm}, \qquad \forall (l,m) \in \mathcal{L}, \forall h \in \mathcal{H}, \tag{29}$$

where we used the results from Lemma 1 to rewrite the constraints in terms of $W_h$.

In the stages $d \in [7]$, we thus solve the problems $C_d(\xi_d, \overline{B}, B_{d-1})$

$$
\begin{aligned}
\min \quad & \sum_{h\in\mathcal{H}}\left[\sum_{g\in\mathcal{G}} f^G_{hg} + \sum_{k\in\mathcal{N}} f^{D+}\left(D^{P+}_{hk}+D^{Q+}_{hk}\right) + f^{D-}\left(D^{P-}_{hk}+D^{Q-}_{hk}\right)\right] + \theta \\
\text{s.t.} \quad & m_{gi}(P^G_{hg}-a_{gi}) + b_{gi} \le f^G_{hg}, && \forall i\in[r_g-1], g\in\mathcal{G}, h\in\mathcal{H} && [\zeta_{hgi}] \\
& (19)-(28) \\
& \begin{bmatrix} -\overline{S}^2_{lm} & \mathbb{Y}_{lm}\bullet W_h & \hat{\mathbb{Y}}_{lm}\bullet W_h \\ \mathbb{Y}_{lm}\bullet W_h & -1 & 0 \\ \hat{\mathbb{Y}}_{lm}\bullet W_h & 0 & -1 \end{bmatrix} \preceq 0, && \forall (l,m)\in\mathcal{L}, \forall h\in\mathcal{H} && [r_{hlm}] \\
& e^0_i + \overline{B}^\top e^1_i + B^\top_{24} e^2_i \le \theta, && \forall i\in[l-1] && [\nu_i] \\
& P^G_{hg}, Q^G_{hg} \ge 0, && \forall g\in\mathcal{G}, \forall h\in\mathcal{H} \\
& B_{hk}, O^+_{hk}, O^-_{hk} \ge 0, && \forall k\in\mathcal{N}^S, \forall h\in\mathcal{H} \\
& D^{P+}_{hk}, D^{P-}_{hk}, D^{Q+}_{hk}, D^{Q-}_{hk} \ge 0, && \forall k\in\mathcal{N}, \forall h\in\mathcal{H} \\
& W_h \succeq 0, && \forall h\in\mathcal{H},
\end{aligned}
$$

where the respective dual multipliers are indicated next to the constraints, $\overline{B}$ is the vector of storage capacities, $B_0 = (B_{0,k})_{k\in\mathcal{N}^S}$ are the initial storage levels, and the value function approximation is described by the intercepts $e^0_i$ and the slopes $e^1_i$ and $e^2_i$. Note that the dual multiplier for the negative semidefiniteness constraints are positive semidefinite matrices $r_{hlm}$ of the form

$$
r = \begin{pmatrix} r^1 & r^2 & r^3 \\ r^2 & r^4 & 0 \\ r^3 & 0 & r^5 \end{pmatrix}.
$$

We denote by $\alpha$ the collection of Lagrange multipliers in the above problem and collect all terms of the Lagrangian that do not contain primary variables in the function

$$
\begin{aligned}
\Gamma_d(\alpha) = & \sum_{h\in\mathcal{H}}\sum_{g\in\mathcal{G}}\left(\sum_{i=1}^{r_g-1}\zeta_{hgi}(b_{gi}-m_{gi}a_{gi}) - \overline{\lambda}_{hg}\overline{P}_g - \overline{\gamma}_{hg}\overline{Q}_g + \underline{\gamma}_{hg}\underline{Q}_g\right) \\
& + \sum_{h\in\mathcal{H}}\sum_{k\in\mathcal{N}}\left(\underline{\mu}_{hk}\underline{V}^2_k - \overline{\mu}_{hk}\overline{V}^2_k + \lambda_{hk}P^D_{hk} + \gamma_{hk}Q^D_{hk}\right) \\
& - \sum_{h\in\mathcal{H}}\sum_{(l,m)\in\mathcal{L}}\left(\overline{S}^2_{lm}r^1_{hlm} + r^4_{hlm} + r^5_{hlm}\right) \\
& - \sum_{k\in\mathcal{N}^S}\left(\sigma_{1k}B_{0,k} + \sum_{h\in\mathcal{H}}\left(\overline{\kappa}_{hk} + \frac{\overline{\beta}^+_{hk}}{4\eta} + \frac{\eta\overline{\beta}^-_{hk}}{4}\right)\overline{B}_k + 0.75\delta_k\overline{B}_k\right) \\
& + \sum_{k\in\mathcal{N}^S}\overline{B}_k\sum_{i\in[l-1]}\nu_i e^1_{ik} + \sum_{i\in[l-1]}\nu_i e^0_i
\end{aligned} \tag{30}
$$

where the terms $0.75\delta_k$ are only required in $d=7$.

In a next step, we define the matrix that contains all the terms that are multiplied with the primal decision variable $W_h$

$$
G_h(\alpha) = \sum_{k\in\mathcal{N}}\left(\lambda_{hk}\mathbb{Y}_k + \gamma_{hk}\hat{\mathbb{Y}}_k + (\overline{\mu}_{hk}-\underline{\mu}_{hk})M_k\right) + \sum_{(l,m)\in\mathcal{L}}\left(2r^2_{hlm}\mathbb{Y}_{lm} + 2r^3_{hlm}\hat{\mathbb{Y}}_{lm}\right)
$$

Using this definition, we can define the dual problem in iteration $l$ in a lattice node as

$$
\max \quad \Gamma_d(\alpha)
$$

$$
\begin{aligned}
\text{s.t.}\quad & G_h(\alpha) \succeq 0 && \forall h \in \mathcal{H} && [W_h]\\
& \sum_{i\in[r_g-1]} \zeta_{hgi} = 1 && \forall g \in \mathcal{G}, \forall h \in \mathcal{H} && [f^G_{hg}]\\
& \sum_{i\in[r_g-1]} \zeta_{hgi} m_{gi} + \overline{\lambda}_{hg} - \lambda_{hk} \geq 0 && \forall k \in \mathcal{N}, \forall g \in \mathcal{G}_k, \forall h \in \mathcal{H} && [P^G_{hg}]\\
& \overline{\gamma}_{hg} - \underline{\gamma}_{hg} - \gamma_{hk} = 0 && \forall k \in \mathcal{N}, \forall g \in \mathcal{G}_k, \forall h \in \mathcal{H} && [Q^G_{hg}]\\
& \sigma_{hk} - \sigma_{h+1,k} + \overline{\kappa}_{hk} \geq 0 && \forall k \in \mathcal{N}^S, \forall h \in [23] && [B_{hk}]\\
& \sigma_{24,k} + \overline{\kappa}_{24,k} + \sum_{i\in[l-1]} \nu_i e^2_{ik} + \delta_k \geq 0 && \forall k \in \mathcal{N}^S && [B_{24,k}]\\
& \lambda_{hk} - \sigma_{hk}\eta + \overline{\beta}^+_{hk} \geq 0 && \forall k \in \mathcal{N}^S && [C^+_{hk}]\\
& -\lambda_{hk} + \sigma_{hk}\frac{1}{\eta} + \overline{\beta}^-_{hk} \geq 0 && \forall k \in \mathcal{N}^S && [C^-_{hk}]\\
& \lambda_{hk} \leq f^{D+}_{hk} && \forall k \in \mathcal{N}, \forall h \in \mathcal{H} && [D^{P+}_{hk}]\\
& \lambda_{hk} \geq -f^{D-}_{hk} && \forall k \in \mathcal{N}, \forall h \in \mathcal{H} && [D^{P-}_{hk}]\\
& \gamma_{hk} \leq f^{D+}_{hk} && \forall k \in \mathcal{N}, \forall h \in \mathcal{H} && [D^{Q+}_{hk}]\\
& \gamma_{hk} \geq -f^{D-}_{hk} && \forall k \in \mathcal{N}, \forall h \in \mathcal{H} && [D^{Q-}_{hk}]\\
& \sum_{i\in[l-1]} \nu_i = 1 && && [\theta]\\
& r_{hlm} \succeq 0 && \forall (l,m) \in \mathcal{L} &&\\
& \nu_i \geq 0, && \forall i \in [l-1] &&\\
& \zeta_{hgi}, \overline{\beta}^-_{hk}, \overline{\beta}^+_{hk}, \overline{\kappa}_{hk}, \overline{\lambda}_{hg}, \overline{\gamma}_{hg}, \underline{\gamma}_{hg}, \overline{\mu}_{hk}, \underline{\mu}_{hk} \geq 0, && \forall k \in \mathcal{N}, \forall g \in \mathcal{G}, \forall h \in \mathcal{H}, &&
\end{aligned}
$$

where the variable $\delta_k$ is only required on the last stage of the problem and can be removed from $\Gamma_d$ and the constraint with dual multiplier $B_{24,k}$ in all other stages.

When solving problem $C_d(\xi_d, \overline{B}, B_{d-1})$ with $d \in 2, \ldots, 7$ in a backward pass for a given state $(\overline{B}, B_0)$, it follows from (30) that the subgradients of $\overline{B}$ and $B_0$ are

$$\left( \sum_{i\in[l-1]} \nu_i e^1_{ik} - \sum_{h\in\mathcal{H}} \left( \overline{\kappa}_{hk} + \frac{\overline{\beta}^+_{hk}}{4\eta} + \frac{\eta\overline{\beta}^-_{hk}}{4} \right) - 0.75\delta_k \right)_{k\in\mathcal{N}^S}$$

and $(-\sigma_{1k})_{k\in\mathcal{N}^S}$, respectively, where again the last term $0.75\delta_k$ is only present in the last stage of the problem. For $d = 1$, the environmental state space only consists of $\bar{B}$ and the subgradient of $\bar{C}_{1l}$ with respect to storage capacity is

$$\left( \sum_{i\in[l-1]} \nu_i e^1_{ik} - \sum_{h\in\mathcal{H}} \left( \overline{\kappa}_{hk} + \frac{\overline{\beta}^+_{hk}}{4\eta} + \frac{\eta\overline{\beta}^-_{hk}}{4} \right) + 0.75(-\sigma_{1k}) \right)_{k\in\mathcal{N}^S}$$

as the initial storage level is 75% of storage capacity.

We conclude this section by showing that the Slater condition holds for the problems on the nodes which implies that there is no duality gap between the primal and dual problem.

PROPOSITION 4. *Strong duality holds between the primal and dual of* $C_d(\xi_d, \bar{B}, B_{d-1})$.

*Proof.* We have to show that the primal problem has a finite optimal value and that the dual problem has a feasible solution in the interior of the feasible set. Clearly, since the demand as well as the production is finite on every lattice node, finiteness of the optimal objective of the primal holds.

To show that the feasible set of the dual problem has an interior point, set

$$\begin{aligned}
&\lambda_{hk} = 0, \quad \zeta_{hgi} = \frac{1}{r_g - 1}, \quad \overline{\lambda}_{hg} = \left| \frac{1}{r_g - 1} \sum_{i \in [r_g - 1]} m_{gi} \right| + 1, \\
&\gamma_{hk} = 0, \quad \overline{\gamma}_{hg} = \underline{\gamma}_{hg} = 1, \\
&\overline{\mu}_{hk} = 2, \quad \underline{\mu}_{hk} = 1 \\
&\sigma_{hk} = 25 - h, \quad \overline{\kappa}_{hk} = 1, \quad \delta_k = 1 \\
&\overline{\beta}^{+}_{hk} = (25 - h)\eta + 1, \quad \overline{\beta}^{-}_{hk} = 1, \quad \nu_i = \frac{1}{l - 1} \\
&r^1_{hlm} = r^4_{hlm} = r^5_{hlm} = 1, \quad r^2_{hlm} = r^3_{hlm} = 0
\end{aligned}$$

for $k \in \mathcal{N}, h \in \mathcal{H}, g \in \mathcal{G}, i \in [r_g - 1]$ and $(l, m) \in \mathcal{L}$. Observe that all variables except $\lambda_{hk}$ and $\gamma_{hk}$, which are not sign constrained, are thus strictly positive.

It is easy to verify that all dual constraints hold and in particular

$$\begin{aligned}
r_{hlm} &= \mathbb{I} \succ 0 \\
G_h(\alpha) &= \sum_{k \in \mathcal{N}} M_k = \mathbb{I} \succ 0,
\end{aligned}$$

establishing that there is a strictly feasible point for the dual problem. □

### 4.3. Numerical Results

We implement the algorithm in MATLAB 2021b and use MOSEK 9.3.10 to solve the optimization problems on the nodes. We approximate $\xi$ using a scenario lattice with 100 nodes per stage. Furthermore, we use YALMIP (Löfberg 2004) to formulate optimization problems and solve problems on nodes in the same stage in the backward pass as well as multiple forward passes for convergence checks in parallel.

In our experiment, we run the algorithm for 100 iterations where in every fifth iteration we increase the number of scenarios in the forward pass to 150 to generate upper bounds on the cost generated by the current policy. All calculations are performed on an Amazon virtual machine of

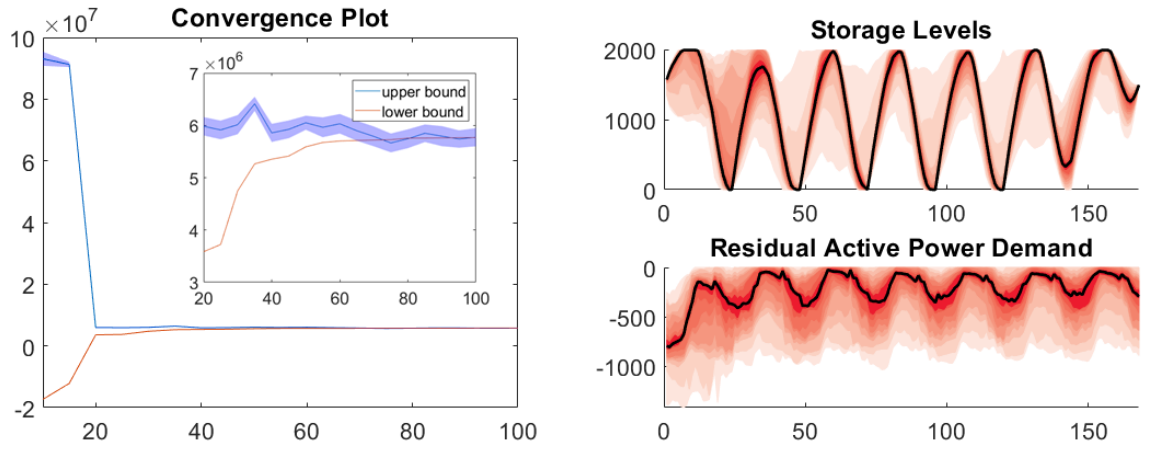


**Figure 4** The panel on the left shows convergence of SDDP upper and lower bound, and a 95% confidence interval for the upper bound. The right panel shows fan plots of the distributions of storage level as well as the residual load on node 122 from 500 scenarios.

the type *c5a.16xlarge* (256 GB, 64 AMD CPU@3.3 GHz) on which the computations took 17.94 hours. Looking at the convergence plot in the left panel of Figure 4, we can observe that the algorithm converges roughly after 60 iterations.

In order to assess the performance of the approach, we generate 500 scenarios and solve the relaxed OPF problem using the approximations of the cost-to-go functions obtained in the last SDDP iteration. We obtain that the optimal storage capacity is equal to 3732 MWh where storage at buses 122 and 119 account for 53% and 28% of the capacity, respectively. As the storage capacity at bus 122 plays a crucial role and the only wind power plant is placed at this bus, we present the operation of this storage on the right panel of Figure 4, where it can be observed that the storage level fluctuates around a regular daily pattern and that the deviations from this pattern are frequent and occasionally substantial.

As the presented approach relies on a convex relaxation of the OPF problem, in some situations optimal decisions $W_h$ do not correspond to physically feasible solutions. To obtain a physically feasible policy for these cases, we solve (17) using the MATLAB function *fmincon* using the *sqp* algorithm and $\delta = 1.25$ to find voltages $\hat{V}_h$ for the 500 forward passes and re-solve the primal nodal problems fixing these voltages as discussed in Section 3.3. We find that the cost for this modified primal problem is only 1.8% (standard deviation 0.0013) higher than the cost when the convex approximation is used, which implies that the dual relaxation of the AC-OPF problem is relatively tight and physically feasible voltages that do not significantly increase cost, can be found using (17). After this operation we obtain a new upper bound of 5.95 mio. (standard deviation 50,982) and thus an optimality gap of 0.19 millions representing 3% of the SDDP lower bound as computed

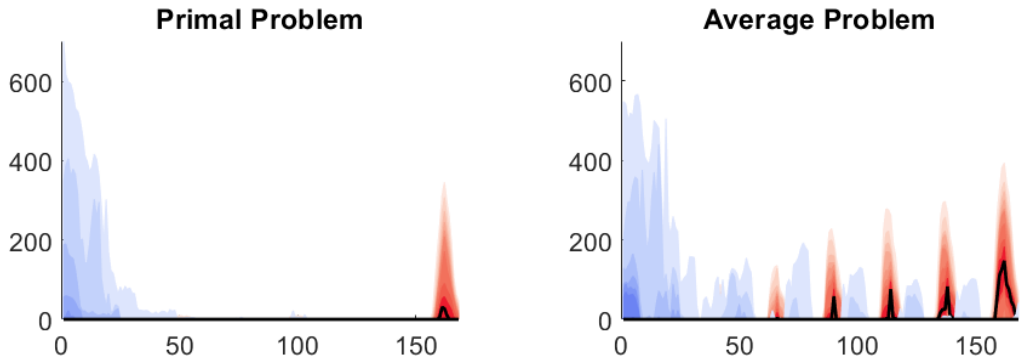


**Figure 5** Comparison of curtailment values for the primal problem and the rolling deterministic approach. Blue and red indicate curtailment of supply and demand respectively.

after 100 iterations.

To compute the value of the stochastic solution, we calculate the value of a rolling horizon deterministic policy, which uses conditional means of the stochastic process to re-optimze decisions in every stage of the problem (see Sethi and Sorger 1991, Schildbach and Morari 2016, Powell 2019, for similar approaches). More specifically, we first solve one large deterministic problem over seven days replacing all stochastic variables by their unconditional means and use the resulting storage investment cost as the cost of the policy in stage 0. We then simulate a random state transition to a lattice node $\hat{\xi}_{1j}$ in stage 1, update the expected realizations of $\xi_d$ for $d \geq 2$ conditional on $\hat{\xi}_{1j}$, re-solve the problem for the 7 days of operation, and use the the cost incurred on day $d = 1$ as the cost of the deterministic policy for that day. We proceed in this manner until the last stage to simulate the overall cost of deterministic planning for the sampled scenario. We repeat this procedure for the 500 scenarios, we used above to test the SDDP policy.

The deterministic benchmark policy invests in 1402 MWh of storage, which is only 37% of the storage capacity bought by the SDDP policy. Comparing curtailed power between the two policies Figure 5 shows that this reduced storage capacity leads to substantially increased curtailment and is therefore suboptimal. This results in an average cost of 7.56 mio (standard deviation $8,362$) which is 27% higher than the optimal cost incurred by the SDDP policy which equals 5.96 (standard deviation $50,982$) million dollars. We can thus conclude that stochastic planning has a substantial added value over state-of-the art deterministic planning approaches.

## 5. Conclusions

We propose the first framework to solve multi-stage stochastic AC-OPF problems. To find solutions to these NP-hard problems, we combine SDDP which allows to efficiently solve Markovian

stochastic programming problems with many stages, with a convex SDP relaxation for AC-OPF problems, which has proven to be of a high quality in deterministic optimization.

We investigate convergence properties of the resulting algorithmic framework and describe how a physically feasible policy that yields a valid upper bound on the original non-convex problem can be obtained. Together with the SDDP lower bound which is valid for the non-convex stochastic AC-OPF problem, an optimality gap can be computed.

In a numerical example on storage sitting, sizing, and operations, we show that the proposed approach is computationally tractable for medium-sized problems and allows to learn policies that have a small optimality gap.

Our numerical results show that the value of the stochastic solution is substantial and therefore stochastic optimization is able to dramatically reduce expected costs in systems with a high share of unpredictable renewable generation.

This paper opens several avenues for further research. Firstly, it would be interesting to extend the problem class to include binary variables in the non-electrical part of the problem, which would enable $(N-1)$ security constrained dispatch and more accurate modeling of technical characteristics of power plants.

Secondly, a speed-up in solving the AC-OPF problems in the nodes could be achieved by partitioning of the admittance matrix for larger networks as in Molzahn et al. (2013), Andersen et al. (2014) or the switch to looser but faster relaxations of the AC-OPF power flow problems in the backward passes, for example, by reformulation as SOCP as in Coffrin et al. (2016), Marley et al. (2017).

Thirdly, a more efficient implementation of SDDP in a low level programming language would help leverage speed-ups from parallelization in the backward pass as well as from quicker set up of optimization problems. Furthermore, an asynchronous version of SDDP would facilitate the distribution of a problem instance amongst several machines in a cluster.

## References

M. Andersen, A. Hansson, and L. Vandenberghe. Reduced-complexity semidefinite relaxations of optimal power flow problems. *IEEE Transactions on Power Systems*, 29(4):1855–1863, 2014.

W. Bai, D. Lee, and K. Lee. Stochastic dynamic ac optimal power flow based on a multivariate short-term wind power scenario forecasting model. *Energies*, 10(12), 2017.

K. Baker, G. Hug, and X. Li. Energy storage sizing taking into account forecast uncertainties and receding horizon operation. *IEEE Transactions on Sustainable Energy*, 8(1):331–340, 2017.

C. Barrows, A. Bloom, A. Ehlen, J. Ikäheimo, J. Jorgenson, D. Krishnamurthy, J. Lau, B. McBennett, M. O'Connell, E. Preston, A. Staid, G. Stephen, and J. Watson. The IEEE reliability test system: A proposed 2019 update. *IEEE Transactions on Power Systems*, 35(1):119–127, 2020.

D. Bienstock and G. Muñoz. On linear relaxations of opf problems. *arXiv preprint arXiv:1411.1120.*, 2014.

D. Bienstock, M. Chertkov, and S. Harnett. Chance-constrained optimal power flow: risk-aware network control under uncertainty. *SIAM Review*, 56(3):461–495, 2014.

J. Birge and F. Louveaux. *Introduction to Stochastic Programming*. Springer Series in Operations Research and Financial Engineering. Springer New York, 2011.

M. Bucciarelli, S. Paoletti, and A. Vicino. Optimal sizing of energy storage systems under uncertain demand and generation. *Applied Energy*, 225:611–621, 2018.

W. Bukhsh, A. Grothey, K. McKinnon, and P. Trodden. Local solutions of the optimal power flow problem. *IEEE Transactions on Power Systems*, 28(4):4780–4788, 2013b.

Y. Cao, Y. Tan, C. Li, and C. Rehtanz. Chance-constrained optimization-based unbalanced optimal power flow for radial distribution networks. *IEEE Transactions on Power Delivery*, 28(3):1855–1864, 2013.

M. Carpentier. Contribution a l erude du dispatching economique. *Bull. de la Soc. Fran. des Elec.*, 8: 431–447, 1962.

A. Castillo, P. Lipka, J.-P. Watson, s. Oren, and R. O'Neill. A successive linear programming approach to solving th iv-acopf. *IEEE Transactions on Power Systems*, 31(4):2752–2763, 2016b.

C. Chen, A. Atamtürk, and S. Oren. Bound tightening for the alternating current optimal power flow problem. *IEEE Transactions on Power Systems*, 31(5):3729–3736, 2016.

N. Chowdhury, F. Pilo, and G. Pisano. Optimal energy storage system positioning and sizing with robust optimization. *Energies*, 13(3), 2020.

C. Coffrin and P. Van Hentenryck. A linear-programming approximations of ac power flows. *INFORMS Journal on Computing*, 26(4):718–734, 2014.

C. Coffrin, H. Hijazi, and P. Van Hentenryck. The qc relaxation: A theoretical and computational study on optimal power flow. *IEEE Transactions on Power Systems*, 31(4):3008–3018, 2016.

C. Coffrin, H. Hijazi, and P. Van Hentenryck. Strengthening the sdp relaxation of ac power flows with

convex envelopes, bound tightening, and valid inequalities. *IEEE Transactions on Power Systems*, 32 (5):3549–3558, 2017.

W. Cole and A. Frazier. Cost Projections for Utility-Scale Battery Storage: 2020 Update. Technical report, National Renewable Energy Laboratory, 2020.

H. Föllmer and A. Schied. *Stochastic Finance: An Introduction in Discrete Time*. De Gruyter studies in mathematics. Walter de Gruyter, 2004.

S. Frank and S. Rebennack. An introduction to optimal power flow: Theory, formulation, and examples. *IIE Transactions*, 48(12):1172–1197, 2016.

S. Frank, I. Steponavice, and S. Rebennack. Optimal power flow: a bibliographic survey i. *Energy systems*, 3(3):221–258, 2012a.

S. Frank, I. Steponavice, and S. Rebennack. Optimal power flow: a bibliographic survey ii. *Energy systems*, 3(3):259–289, 2012b.

D. Gayme and U. Topcu. Optimal power flow with large-scale storage integration. *IEEE Transactions on Power Systems*, 28(2):709–717, 2013.

P. Girardeau, V. Leclere, and A. B. Philpott. On the convergence of decomposition methods for multistage stochastic convex programs. *Mathematics of Operations Research*, 40(1):130–145, 2015.

J. Glover, M. Sarma, and T. Overbye. *Power system analysis and design*. Australia: Thomson, 2008.

G. Hanasusanto, D. Kuhn, and W. Wiesemann. A comment on "computational complexity of stochastic programming problems". *Mathematical Programming*, 159(1):557–569, Sep 2016.

H. Heitsch and W. Römisch. Scenario tree modeling for multistage stochastic programs. *Mathematical Programming*, 118:371–406, 2009.

N. Helistö, J. Kiviluoma, J. Ikäheimo, T. Rasku, E. Rinne, C. O'Dwyer, R. Li, and D. Flynn. Backbone—an adaptable energy systems modelling framework. *Energies*, 12(17):3388, 2019.

R. Jabr. Radial distribution load flow using conic programming. *IEEE Transactions on Power Systems*, 21 (3):1458–1459, 2006.

R. Jabr, S. Karaki, and J. Korbane. Robust multi-period opf with storage and renewables. *IEEE Transactions on Power Systems*, 30(5):2790–2799, 2015.

C. Josz, J. Maeght, P. Panciatici, and J. Gilbert. Application of the moment-sos approach to global optimization of the opf problem. *IEEE Transactions on Power Systems*, 30(1):463–470, 2015.

A. Kargarian, G. Hug, and J. Mohammadi. A multi-time scale co-optimization method for sizing of energy storage and fast-ramping generation. *IEEE Transactions on Sustainable Energy*, 7(4):1351–1361, 2016.

A. Kiszka and D. Wozabal. A stability result for linear Markovian stochastic optimization problems. *Mathematical Programming*, 2020.

B. Kocuk, S. Dey, and X. Sun. Strong socp relaxations for the optimal power flow problem. *Operations Research*, 64(6):1177–1196, 2016b.

B. Kocuk, S. Dey, and X. Sun. Matrix minor reformulation and socp-based spatial branch-and-cut method for the ac optimal power flow problem. *Mathematical Programming*, pages 557–593, 2018.

G. Lan. Complexity of stochastic dual dynamic programming. *Mathematical Programming*, pages 1–38, 2020.

D. Larrahondo, R. Moreno, H. R. Chamorro, and F. Gonzalez-Longatt. Comparative performance of multi-period acopf and multi-period dcopf under high integration of wind power. *Energies*, 14(15), 2021.

J. Lavaei and S. H. Low. Zero duality gap in optimal power flow problem. *IEEE Transactions on Power Systems*, 27(1):92–107, 2012.

J. Löfberg. Yalmip : A toolbox for modeling and optimization in matlab. In *In Proceedings of the CACSD Conference*, Taipei, Taiwan, 2004.

N. Löhndorf and D. Wozabal. Gas storage valuation in incomplete markets. *European Journal of Operational Research*, 280(1):318 – 330, 2021.

N. Löhndorf, D. Wozabal, and S. Minner. Optimizing trading decisions for hydro storage systems using approximate dual dynamic programming. *Operations Research*, 61(4):810–823, 2013.

S. Low. Convex relaxation of optimal power flow part i: Formulations and equivalence. *IEEE Transactions on Control of Network Systems*, 1(1):15–27, 2014a.

S. Low. Convex relaxation of optimal power flow part ii: Exactness. *IEEE Transactions on Control of Network Systems*, 1(2):177–189, 2014b.

R. Madani, S. Sojoudi, and J. Lavaei. Convex relaxation for optimal power flow problem: mesh networks. *IEEE Transactions on Power Systems*, 30(1):199–211, 2015b.

R. Madani, M. Ashraphijuo, and J. Lavaei. Promises of conic relaxation for contingency-constrained optimal power flow problem. *IEEE Transactions on Power Systems*, 31(2):1297–1307, 2016.

J. Marley, D. Molzahn, and I. Hiskens. Solving multiperiod opf problems using an ac-qp algorithm initialized with an socp relaxation. *IEEE Transactions on Power Systems*, 32(5):3538–3548, 2017.

I. Mezghani, S. Misra, and S. Deka. Stochastic ac optimal power flow: A data-driven approach. *Electric Power Systems Research*, 189:106567, 2020.

M. Miletić, H. Pandžić, and D. Yang. Operating and investment models for energy storage systems. *Energies*, 13(18), 2020.

S. Misra, D. Molzahn, and K. Dvijotham. Optimal adaptive linearizations of the ac power flow equations. In *2018 Power Systems Computation Conference (PSCC)*, pages 1–7. IEEE, 2018.

B. Mo, A. Gjelsvik, and A. Grundt. Integrated risk management of hydro power scheduling and contract management. *IEEE Transactions on Power Systems*, 16(2):216–221, 2001.

D. Molzahn and I. Hiskens. Sparsity-exploiting moment-based relaxations of the optimal power flow problem. *IEEE Transactions on Power Systems*, 30(6):3168–3180, 2015c.

D. Molzahn and I. Hiskens. A survey of relaxations and approximations of the power flow equations. *Foundations and Trends in Electric Energy Systems*, 4(1-2):1–221, 2019.

D. Molzahn, J. Holzer, B. Lesieutre, and C. DeMarco. Implementation of a large-scale optimal power flow solver based on semidefinite programming. *IEEE Transactions on Power Systems*, 28(4):3987–3998, 2013.

D. Molzahn, J. Holzer, and B. Lesieutre. Convex relaxations of optimal power flow problem: an illustrative example. *Transactions on Circuits and Systems I: Regular Papers*, 63(5):650–660, 2016.

T. Mühlpfordt, T. Faulwasser, and V. Hagenmeyer. Solving stochastic ac power flow via polynomial chaos expansion. *2016 IEEE Conference on Control Applications (CCA)*, pages 70–76, 2016.

K. Natarajan, D. Shi, and K.-C. Toh. A penalized quadratic convex reformulation method for random quadratic unconstrained binary optimization. *Optimization Online*, pages 1–26, 2013.

M. Nick, R. Cherkaoui, and M. Paolone. Optimal allocation of dispersed energy storage systems in active distribution networks for energy balance and grid support. *IEEE Transactions on Power Systems*, 29 (5), 2014.

H. Oh. Optimal planning to include storage devices in power systems. *IEEE Transactions on Power Systems*, 26(3):1118–1128, 2011.

H. Pandzic, Y. Wang, T. Qiu, Y. Dvorkin, and D. Kirschen. Near-optimal method for siting and sizing of distributed storage in a transmission network. *IEEE Transactions on Power Systems*, 30(5):2288–2300, 2015.

M. Pereira and L. Pinto. Multi-stage stochastic optimization applied to energy planning. *Mathematical Programming*, 52(2):359–375, 1991.

G. C. Pflug and A. Pichler. *Multistage Stochastic Optimization*. Springer Series in Operations Research and Financial Engineering, 2014.

G. C. Pflug and W. Römisch. *Modeling, Measuring and Managing Risk*. World Scientific, August 2007.

D. Phan. Lagrange duality and branch-and-bound algorithm for optimal power flow. *Operations Research*, 60(2):275–285, 2012.

A. Philpott and V. de Matos. Dynamic sampling algorithms for multi-stage stochastic programs with risk aversion. *European Journal of Operational Research*, 218(2):470 – 483, 2012.

A. Philpott and Z. Guan. On the convergence of stochastic dual dynamic programming and related methods. *Operations Research Letters*, 36(4):450–455, 2008.

W. Powell. A unified framework for stochastic optimization. *European Journal of Operational Research*, 275 (3):795–821, 2019.

T. Qiu, B. Xu, Y. Wang, Y. Dvorkin, and D. Kirschen. Stochastic multistage coplanning of transmission expansion and energy storage. *IEEE Transactions on Power Systems*, 32(1):643–651, 2017.

S. Reddy. Optimal power flow with renewable energy resources including storage. *Electrical Engineering*, 99 (2):685–695, 2017.

L. Roald and G. Andersson. Chance-constrained ac optimal power flow: Reformulations and efficient algorithms. *IEEE Transactions on Power Systems*, 33(3):2906–2918, 2018.

D. Schetinin. Efficient bound tightening techniques for convex relaxations of ac optimal power flow. *IEEE Transactions on Power Systems*, 34(5):3848–3857, 2019.

G. Schildbach and M. Morari. Scenario-based model predictive control for multi-echelon supply chain management. *European Journal of Operational Research*, 252(2):540–549, 2016.

S. Sethi and G. Sorger. A theory of rolling horizon decision making. *Annals of Operations Research*, 29(1): 387–415, 1991.

A. Shapiro. Analysis of stochastic dual dynamic programming method. *Eur J Oper Res*, 209(1):63–72, 2011.

A. Shapiro, D. Dentcheva, and A. Ruszczyński. *Lectures on Stochastic Programming: Modeling and Theory*. MOS-SIAM series on optimization. Society for Industrial and Applied Mathematics, 2009.

H. Sharifzadeh, N. Amjady, and H. Zareipour. Multi-period stochastic security-constrained opf considering the uncertainty sources of wind power, load demand and equipment unavailability. *Electric Power Systems Research*, 146:33–42, 2017.

D. Shchetinin, T. De Rubira, and G. Hug-Glanzmann. On the construction of linear approximations of lie flow constraints for ac optimal power flow. *IEEE Transactions on Power Systems*, 34(2):1182–1192, 2018.

B. Stott, J. Jardim, and O. Alsac. DC Power Flow Revisited. *IEEE Trans. Power Syst.*, 24(3):1290–1300, 2009.

G. Terça and D. Wozabal. Envelope Theorems for Multi-Stage Linear Stochastic Optimization. *Operations Research*, 2020.

M. Vrakopoulou, K. Margellos, J. Lygeros, and G. Andersson. Probabilistic guarantees for the n-1 security of systems with wind power generation. In *Reliability and Risk Evaluation of Wind Integrated Power Systems. Reliable and Sustainable Electric Power and Energy Systems Management*, pages 59–73. Springer India, 2013.

G. Wang and H. Hijazi. Mathematical programming methods for microgrid design and operations: a survey on deterministic and stochastic approaches. *Computational Optimization and Applications*, 71:553–608, 2018.

W. Wei, J. Wang, N. Li, and S. Mei. Optimal power flow of radial networks and its variations: A sequential convex optimization approach. *IEEE Transactions on Smart Grid*, 8(6):2974–2987, 2017.

S. Wogrin and D. Gayme. Optimizing storage siting, sizing, and technology portfolios in transmission-constrained networks. *IEEE Transactions on Power Systems*, 30(6):3304–3313, 2015.

D. Wu, D. Molzahn, B. Lesieutre, and K. Dvijotham. A deterministic method to identify multiple local

extrema for the ac optimal power flow problem. *IEEE Transactions on Power Systems*, 33(1):654–668, 2018a.

P. Xiong and C. Singh. Optimal planning of storage in power systems integrated with wind power generation. *IEEE Transactions on Sustainable Energy*, 7(1):232–240, 2016.

R. Zafar, J. Ravishankar, J. Fletcher, and H. Pota. Optimal dispatch of battery energy storage system using convex relaxations in unbalanced distribution grids. *IEEE Transactions on Industrial Informatics*, 16 (1):97–108, 2020.

H. Zhang and P. Li. Chance constrained programming for optimal power flow under uncertainty. *IEEE Transactions on Power Systems*, 26(4):2417–2424, 2011.

Y. Zhang, S. Shen, and J. Mathieu. Distributionally robust chance-constrained optimal power flow with uncertain renewables and uncertain reserves provided by loads. *IEEE Transactions on Power Systems*, 32(2):1378–1388, 2017.

M. Zidar, P. S. Georgilakis, N. D. Hatziargyriou, T. Capuder, and D. Škrlec. Review of energy storage allocation in power distribution networks: applications, methods and future research. *IET Generation, Transmission Distribution*, 10(3):645–652, 2016.

F. Zohrizadeh, C. Josz, M. Jin, R. Madani, J. Lavaei, and S. Sojoudi. A survey on conic relaxations of optimal flow problem. *European Journal of Operational Research*, 287(2):391–409, 2020.

## Appendix A: Proofs

### A.1. Proof of Lemma 1

We start by noting that for any vector $x \in \mathbb{R}^n$ and matrix $A \in \mathbb{R}^{n\times n}$ the following holds

$$x^\top Ax = x^\top \left(\frac{2A}{2}\right) x = \frac{x^\top Ax + x^\top Ax}{2} = \frac{x^\top Ax + x^\top A^\top x}{2} = x^\top \left(\frac{A+A^\top}{2}\right) x. \tag{31}$$

We also note that for a matrix $A \in \mathbb{C}^{n\times n}$ and a vector $y \in \mathbb{C}^n$, we have

$$\begin{aligned} Ay &= (\mathfrak{Re}(A) + i\mathfrak{Im}(A))(\mathfrak{Re}(y) + i\mathfrak{Im}(y)) \\ &= (\mathfrak{Re}(A)\mathfrak{Re}(y) - \mathfrak{Im}(A)\mathfrak{Im}(y)) + i(\mathfrak{Re}(A)\mathfrak{Im}(y) + \mathfrak{Im}(A)\mathfrak{Re}(y)) \end{aligned}$$

By (31), this implies that

$$\widetilde{Ay} = \begin{pmatrix} \mathfrak{Re}(A) & -\mathfrak{Im}(A) \\ \mathfrak{Im}(A) & \mathfrak{Re}(A) \end{pmatrix} \tilde{y} \quad \text{and} \quad \mathfrak{Re}(y^H Ay) = \tilde{y}^\top \begin{pmatrix} \mathfrak{Re}(A) & -\mathfrak{Im}(A) \\ \mathfrak{Im}(A) & \mathfrak{Re}(A) \end{pmatrix} \tilde{y} = \tilde{y}^\top \mathbb{A} \tilde{y}, \tag{32}$$

which is what we used to prove in the formula for real power in Section 2.4.

Turning to injected imaginary power, we obtain for similar reasons

$$\mathfrak{Im}(y^H Ay) = \tilde{y}^\top \begin{pmatrix} \mathfrak{Im}(A) & \mathfrak{Re}(A) \\ -\mathfrak{Re}(A) & \mathfrak{Im}(A) \end{pmatrix} \tilde{y} = -\tilde{y}^\top \tilde{\mathbb{A}} \tilde{y} \tag{33}$$

Starting from the equality for injected reactive power, we obtain

$$\begin{aligned} Q_{tk} &= \mathfrak{Im}(V_{tk} I_{tk}^*) = -\mathfrak{Im}(V_{tk}^* I_{tk}) = -\mathfrak{Im}(V_t^H e_k e_k^\top I_t) = -\mathfrak{Im}(V_t^H Y_k V_t) \\ &= \tilde{V}_t^\top \hat{\mathbb{Y}}_k \tilde{V}_t = \mathrm{tr}(\tilde{V}_t^\top \hat{\mathbb{Y}}_k \tilde{V}_t) = \mathrm{tr}(\hat{\mathbb{Y}}_k \tilde{V}_t \tilde{V}_t^\top) = \mathrm{tr}(\hat{\mathbb{Y}}_k W_t) = \hat{\mathbb{Y}}_k \bullet W_t, \end{aligned}$$

where the second equality follows from $\mathfrak{Im}(V_{tk} I_{tk}^*) = -\mathfrak{Im}(V_{tk}^* I_{tk})$, the fourth from $I_t = YV_t$ and the definition of $Y_k = e_k e_k^\top Y$ and the rest from (33) and the properties of the trace.

For the squared voltage, we get

$$|V_{tk}|^2 = V_{tk}^* V_{tk} = V_t^H e_k e_k^\top V_t = \tilde{V}_t^\top M_k \tilde{V}_t = \mathrm{tr}(M_k \tilde{V}_t \tilde{V}_t^\top) = M_k \bullet W_t.$$

To prove relations for lines, we recall the definitions in (4) via $Y_{lm}$

$$\begin{aligned} |I_{tlm}|^2 &= (e_l^\top Y_{lm} V_t)^H (e_l^\top Y_{lm} V_t) = (Y_{lm} V_t)^H (Y_{lm} V_t) = (\mathbb{Y}_{lm} \tilde{V}_t)^\top (\mathbb{Y}_{lm} \tilde{V}_t) = \tilde{V}_t^\top \mathbb{Y}_{lm}^\top \mathbb{Y}_{lm} \tilde{V}_t \\ &= \mathrm{tr}(\mathbb{Y}_{lm}^\top \mathbb{Y}_{lm} \tilde{V}_t \tilde{V}_t^\top) = \mathbb{Y}_{lm}^\top \mathbb{Y}_{lm} \bullet W_t \\ |S_{tlm}|^2 &= \mathfrak{Re}(V_t^H Y_{lm} V_t)^2 + \mathfrak{Im}(V_t^H Y_{lm} V_t)^2 = (\mathbb{Y}_{lm} \bullet W_t)^2 + (\hat{\mathbb{Y}}_{lm} \bullet W_t)^2 \end{aligned}$$

and the result about the active power on the line immediately follows. Finally, the relation for voltage difference can be proven in the same way as for the squared voltage

$$\begin{aligned} |V_{tl} - V_{tm}|^2 &= (V_{tl} - V_{tm})^* (V_{tl} - V_{tm}) = V_t^H (e_l - e_m)(e_l - e_m)^T V_t = \tilde{V}_t^T M_{lm} \tilde{V}_t \\ &= \mathrm{tr}(M_{lm} \tilde{V}_t \tilde{V}_t^T) = M_{lm} \bullet W_t. \end{aligned}$$

### A.2. Proof of Proposition 3

Denote by $\mathcal{K}_l$ the normed eigenvectors of $W_t$ with positive eigenvalues. Since

$$\operatorname{tr}(G(\alpha)W_t)$$

is part of the Lagrangian, it has to hold that for every $\mathcal{K}_l$

$$G(\alpha)\mathcal{K}_l = 0,$$

i.e., that $\mathcal{K}_l$ is in the null space of $G(\alpha)$. If this would not be the case, then one could choose a $W_t'$ such that the eigenvalue of $\mathcal{K}_l$ is zero thereby reducing the objective of the inner optimization problem in the Lagrangian, leading to a contradiction to the optimality of $W_t$.

Therefore if the dimension of kernel of $G(\alpha)$ is at most two, there are at most 2 linearly independent eigenvecors of $W_t$ with positive eigenvalues. If there is only one, then $W_t = \tilde{V}_t\tilde{V}^\top$ for some vector $\tilde{V}_t$ whose components can be directly interpreted as voltages. In case there are two, we note that by the structure of $\mathbb{Y}_k$ and $\hat{\mathbb{Y}}_k$, the matrix $G(\alpha^*)$ has the form

$$G(\alpha)) = \begin{pmatrix} T(\alpha) & \bar{T}(\alpha) \\ -\bar{T}(\alpha) & T(\alpha) \end{pmatrix},$$

for some matrices $T$ dependent on $\alpha$.

Therefore, if $\mathcal{K} = (\mathcal{K}_1^\top, \mathcal{K}_2^\top)^\top$ is one of the two eigenvectors, then the orthogonal vector $\mathcal{K}_\perp = (-\mathcal{K}_2^\top, \mathcal{K}_1^\top)^\top$ also has a non-zero eigenvalue, since $G(\alpha)\mathcal{K}_\perp$ yields a the same vector as $G(\alpha)\mathcal{K}$ with flipped components. We can therefore conclude that

$$W_t = \rho_1\mathcal{K}\mathcal{K}^\top + \rho_2\mathcal{K}_\perp\mathcal{K}_\perp^\top.$$

Since for any matrix $A$ of the general form of $G$ it holds that $\operatorname{tr}(A\mathcal{K}\mathcal{K}^\top) = \operatorname{tr}(A\mathcal{K}_\perp\mathcal{K}_\perp^\top)$, for a given choice of the other primal and dual variables the rank 1 matrix

$$W_t^\star = (\rho_1 + \rho_2)\mathcal{K}\mathcal{K}^\top$$

yields the same results as $W_t$ in the constraints of $\bar{C}_{tl}(\xi_{tn}, X_{t-1})$ and therefore is a feasible solution with the same objective as $W_t$. This proves the first point of the proposition.

To prove the second point, we have to find the vector $\tilde{V}_t = (\tilde{V}_{t1}, \tilde{V}_{t2})^\top$ in the null space of $G(\alpha)$ whose components can be be interpreted as the real and imaginary component of the voltage vector such that $\tilde{V}_t\tilde{V}_t^\top$ is the physically correct rank one solution of the problem.

To find such a vector, we find parameters $g_1,\ g_2 \in \mathbb{R}$ such that

$$\tilde{V}_t = g_1\begin{pmatrix}\mathcal{K}_1 \\ \mathcal{K}_2\end{pmatrix} + g_2\begin{pmatrix}-\mathcal{K}_2 \\ \mathcal{K}_1\end{pmatrix}$$

and the reconstructed voltages

$$V_t^\star = (g_1\mathcal{K}_1 - g_2\mathcal{K}_2) + i(g_1\mathcal{K}_2 + g_2\mathcal{K}_1)$$

fit the known voltages at nodes $m_1$ and $m_2$, i.e.,

$$\mathfrak{Re}(V_{t,m_1}) = g_1\mathcal{K}_{1,m_1} - g_2\mathcal{K}_{2,m_1}, \quad \mathfrak{Im}(V_{t,m_2}) = g_2\mathcal{K}_{1,m_2} + g_1\mathcal{K}_{2,m_2},$$

which finishes the proof. □

## Appendix B: Additional Material on AC Power Flow

### B.1. Phase-Shifting Transformers with Off-Nominal Turns Ratios

As outlined in Section 2.1, current that flows through a conductor induces a magnetic field which increases in strength with the amount of current and if the conductor is wound up in a coil. In an AC network, the magnetic field therefore pulsates and changes polarity along with the current.

This electromagnetic effect works *in both directions*, i.e., if magnetic field lines are moved over an conductor a current is induced. Hence, if a second coil is placed in close proximity to a coil for which a fluctuating magnetic field is induced by AC current passing through the coil, the field induces an AC current in the second coil because the change in intensity and direction of the magnetic field constantly disturbs the free electrons in the second coil and forces them to move.

This is the basic principle of a transformer which converts an AC voltage in the primary coil *in front* of the transformer to a different AC voltage in the secondary coil *behind* the transformer. Note that if the coils would just be placed next to another, a significant part of the magnetic field from the primary side would not be *in range* of the secondary coil. Therefore in real transformers a core of ferromagnetic material is placed in loop between primary and secondary coils to prevent wastage of energy.

The change of voltage between the primal and secondary coil depends on the *turns ratio* of the two coils and for an ideal transformer (without any losses) it can be expressed as

$$\frac{V_1}{V_2} = \frac{N_1}{N_2} = \frac{I_2}{I_1}$$

where $N_1$ and $N_2$ are the numbers of turns of the respective coils and $V_1$, $I_1$ an $V_2$, $I_2$ are the primary and secondary voltages and currents, respectively.

It follows that the induced voltage in the secondary coil $V_2 = V_1 \frac{N_2}{N_1}$ increases in the primary voltage and in the proportion of turns in the secondary coil to the primary one. Hence, $V_2$ can be *stepped up* by using more windings in the secondary coil and *stepped down* by using less windings. While higher voltages $V_2$ imply lower currents $I_2$ (by the conservation of power) and therefore lower transmission losses (which are proportional to current), lower voltages are safer to handle

and therefore more suitable for end-consumers. The ability to easily switch between voltage levels using transformers is one of the main advantages of AC current over DC current and the reason why AC technology is used in contemporary electric grids.

We distinguish transformers with nominal and off-nominal turns ratio. When the ratio of selected voltage bases for the per-unit system on either side of the transformer is equal to the turns ratio, the transformer is called a transformer with *nominal turns ratio*. In such situation the transformer can effectively be eliminated from power flow calculations as voltages, currents, external impedances, and admittances expressed in the per-unit system do not change when they are referred from one side of a transformer to the other. Taking voltages as an example, we see that

$$\frac{V_{1,p.u.}}{V_{2,p.u.}} = \frac{\frac{V_1}{V_{1,base}}}{\frac{V_2}{V_{2,base}}} = \frac{V_1}{V_2}\frac{V_{2,base}}{V_{1,base}} = \frac{N_1}{N_2}\frac{N_2}{N_1} = 1$$

for a transformer with nominal turns ratio.

However, in some cases it is impossible to select voltage bases in this manner – see Glover et al. (2008) for an example of two parallel transformers where this is the case. Such transformers have *off-nominal turns ratios* and require correction to the admittance matrix to account for the additional voltage magnitude $T$ relative to the nominal case, i.e.,

$$\frac{N_1}{N_2} = \frac{V_{1,base}}{V_{2,base}}T.$$

This implies that when we are operating in per-unit system, the *effective turns ratio*, i.e., the factor of proportionality between the two per unit voltages, equals $T$, since

$$\frac{V_{1,p.u.}}{V_{2,p.u.}} = \frac{V_1}{V_2}\frac{V_{2,base}}{V_{1,base}} = \frac{N_1}{N_2}\frac{V_{2,base}}{V_{1,base}} = \frac{V_{1,base}}{V_{2,base}}T\frac{V_{2,base}}{V_{1,base}} = T.$$

Apart from transformers having off-nominal turns ratio, another complication relative to the simple situation described in Section 2 is that transformers can be used to control the phase angle. Such transformers are called *phase-shifting transformers* and are modeled by a (hypothetical) complex turns ratio $e^{i\phi}$, which allows to represent a phase shift $\phi$ for transformers in power flow calculations.

To sum up, consider a phase-shifting transformer with off-nominal turns ratio represented by a magnitude $T_{lm}$ and a phase shift $\phi_{lm}$ and assume that the transformer is placed on the line $(l, m)$ and assigned to bus $l$. Then the effective turns ratio of the transformer is

$$\frac{V_l}{V_{l'}} = T_{lm}e^{i\phi_{lm}}.$$

where $l$ and $l'$ refer to the left and right side of the transformer respectively as presented on Figure 6 and $V_l$ and $V_{l'}$ represent voltage values in per-unit system just before and just after the current

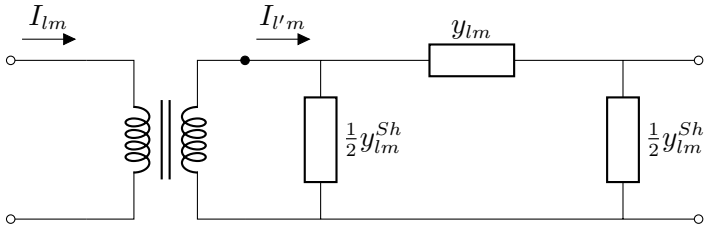


**Figure 6** Graph presents two buses connected with the line including transformer and respective admittances.

passes through the transformer. Note that $l'$ acts as a new node in the network and we will see below how to get rid of it again for the price of an asymmetric admittance matrix.

Since the power loss is negligible in the ideal transformer, we have

$$V_l I_{lm}^* = V_{l'} I_{l'm}^*$$

where $I_{lm}$ is the current flowing through line $(l, m)$ from bus $l$ to $m$, which implies

$$\frac{I_{lm}}{I_{l'm}} = \left(\frac{V_{l'}}{V_l}\right)^* = \left(\frac{1}{T_{lm}e^{i\phi_{lm}}}\right)^* = \frac{1}{T_{lm}e^{-i\phi_{lm}}}. \tag{34}$$

## B.2. The Admittance Matrix

In Section 2, we discuss a simple form of the admittance matrix, which does neither take into account shunt admittances of lines nor phase-shifting transformers or transformers with off-nominal turns ratios. While this simpler view is sufficient for modeling many power systems, we discuss the general case here, since it is required for our application example in Section 4.

We start by noting that besides busses, branches may also have a shunt admittance $y_{lm}^{Sh}$ (also called total charging susceptance) representing leakage of current from within the branch $(l, m)$ to the reference node. As is common, we apply this admittance equally to the busses at the end of the branch to incorporate leakage along the branch.

Furthermore, we assume that there is a transformer represented by magnitude $T_{lm}$ and phase shift $\phi_{lm}$ placed at the branch $(l, m)$ and assigned to bus $l$ (see Figure 6).

To model this situation, we start by applying Kirchhoffs's current law to node $l'$ behind the transformer. Since there are no losses associated to the transformer, the current flowing into $l'$ is just $I_{l'm}$. To transform this current into the per-unit system *in front* the transformer and thereby eliminate $l'$, we use (34) to write $I_{l'm} = I_{lm}T_{lm}e^{-i\phi_{lm}}$. The current flowing out of node $l'$ is on the one hand the current lost due to half of the shunt admittance, which due to Ohm's law, can be written as $V_{l'}\frac{1}{2}y_{lm}^{Sh}$ and the current that flows from $l'$ to $m$, which is $(V_{l'} - V_m)y_{lm}$. In summary, we can write

$$0 = I_{lm}T_{lm}e^{-i\phi_{lm}} - V_{l'}\frac{1}{2}y_{lm}^{Sh} - (V_{l'} - V_m)y_{lm}$$

which can be re-written as

$$\begin{aligned} I_{lm} &= (T_{lm}e^{-i\phi_{lm}})^{-1}\left(V_{l'}\frac{1}{2}y_{lm}^{Sh} + (V_{l'} - V_m)y_{lm}\right) \\ &= (T_{lm}e^{-i\phi_{lm}})^{-1}\left(\left(y_{lm} + \frac{1}{2}y_{lm}^{Sh}\right)V_{l'} - y_{lm}V_m\right) \\ &= (T_{lm}e^{-i\phi_{lm}})^{-1}\left(\left(y_{lm} + \frac{1}{2}y_{lm}^{Sh}\right)\frac{1}{T_{lm}e^{i\phi_{lm}}}V_l - y_{lm}V_m\right) \\ &= \frac{1}{T_{lm}^2}\left(y_{lm} + \frac{1}{2}y_{lm}^{Sh}\right)V_l - \frac{1}{T_{lm}e^{-i\phi_{lm}}}y_{lm}V_m, \end{aligned} \tag{35}$$

where in the third line we used the definition of $V_{l'}$ in terms of $V_l$ in order to eliminate the node $l'$ from the equation and $y_{lm}$ is series admittance of the line $(l,m)$.

Similarly, we can use Kirchhoff's current law for $(m,l)$, which, expressed in the per-unit system of bus $m$, yields

$$0 = I_{ml} - V_m\frac{1}{2}y_{lm}^{Sh} - (V_m - V_{l'})y_{lm}$$

which we can re-arrange to

$$I_{ml} = \left(y_{lm} + \frac{1}{2}y_{lm}^{Sh}\right)V_m - \frac{1}{T_{lm}e^{i\phi_{lm}}}y_{lm}V_l. \tag{36}$$

Inspecting (35) and (36) it becomes clear that allowing for transformers with off-nominal turns ratios and non-zero phase shifts introduces an asymmetry in the admittance matrix, when using the per-unit system. In order to deal with this in the definition of the admittance matrix, we define $\tilde{\mathcal{L}} = \mathcal{L} \cup \{(m,l) : (l,m) \in \mathcal{L}\}$ and set $y_{ml} = y_{lm}, y_{ml}^{Sh} = y_{lm}^{Sh}, T_{ml} = 1, \phi_{ml} = -\phi_{lm}$ for every $(l,m) \in \mathcal{L}$ with the transformer assigned to the bus $l$.

In order to define the partial admittance matrix $Y_{lm}$ in the presence of phase shifting transformers with off-nominal turns ratios and shunt admittances, we write

$$Y_{lm} = \frac{1}{T_{lm}^2}\left(y_{lm} + \frac{1}{2}y_{lm}^{Sh}\right)e_l e_l^\top - \frac{1}{T_{lm}T_{ml}e^{-i\phi_{lm}}}y_{lm}e_l e_m^\top, \quad \forall (l,m) \in \tilde{\mathcal{L}}.$$

Note that for the above definition $I_{lm} = e_l^T Y_{lm} V$ and $I_{ml} = e_m^T Y_{ml} V$ are satisfied.

Finally, to derive the relationships between voltage and current on the busses in the setting of this section, based on Ohm's law and Kirchoff's current law we write

$$\begin{aligned} I_k &= I_{k0} + \sum_{j:(k,j)\in\tilde{\mathcal{L}}} I_{kj} = y_k V_k + \sum_{j:(k,j)\in\tilde{\mathcal{L}}}\left(\frac{1}{T_{kj}^2}\left(y_{kj} + \frac{1}{2}y_{kj}^{Sh}\right)V_k - \frac{1}{T_{kj}T_{jk}e^{-i\phi_{kj}}}y_{kj}V_j\right) \\ &= \left(y_k + \sum_{j:(k,j)\in\tilde{\mathcal{L}}}\frac{1}{T_{kj}^2}\left(y_{kj} + \frac{1}{2}y_{kj}^{Sh}\right)\right)V_k + \sum_{j:(k,j)\in\tilde{\mathcal{L}}}\left(-\frac{1}{T_{kj}T_{jk}e^{-i\phi_{kj}}}y_{kj}\right)V_j \end{aligned}$$

for every $k \in \mathcal{N}$. In order to represent this in the compact form $I = YV$ as in Section 2.1, we define the elements of the admittance matrix $Y$ as

$$(Y)_{kk} = y_k + \sum_{j:(k,j)\in\tilde{\mathcal{L}}} \frac{1}{T_{kj}^2}\left(y_{kj} + \frac{1}{2}y_{kj}^{Sh}\right),$$
$$(Y)_{kj} = -\sum_{(k,j)\in\tilde{\mathcal{L}}} \frac{1}{T_{kj}T_{jk}e^{-i\phi_{kj}}} y_{kj}, \quad j \neq k.$$